Research Article

Nneka Joyce Odimba, Reza Khalidy, Reza Bakhshoodeh, and Rafael M. Santos*

Recovery of critical metals from carbonatite-type mineral wastes: Geochemical modeling investigation of (bio)hydrometallurgical leaching of REEs

https://doi.org/10.1515/gps-2022-8086
received July 25, 2022; accepted March 05, 2023

Abstract: Rare earth elements (REEs) are typically found in low concentrations within natural rocks that make up mine tailings, such as carbonates in association with silicates within carbonatite igneous rocks, so it is of interest to develop (bio)hydrometallurgical ways to liberate them from the silicate matrix. This work investigated, through geochemical modeling, the extraction of europium and ytterbium carbonates from rocks containing one of four silicates (chrysotile, forsterite, montmorillonite, and phlogopite) via chemical (mineral acid) or biological (organic acid) leaching. The results indicated conditions that led to either congruent or incongruent dissolution of the mineral phases and the formation of transient mineral phases. Chemical leaching models suggest that REE carbonates are recoverable in one-step leaching from forsterite and chrysotile rocks, while they are recoverable in a secondary leaching step from montmorillonite and phlogopite rocks. Gibbsite as a transient phase is shown to complicate REE recovery, potentially requiring reactive extraction. REEs have the potential to be recovered from silicate rocks via chemoorganotrophic bioleaching, but the process configuration would differ depending on the predominant minerals that make up the rock, and the type of REE present in it.

Keywords: green chemistry raw materials, mine waste valorization, mineral dissolution and precipitation, acid leaching

1 Introduction

The function of collection, transfer, recovery, recycling, and reusing of waste is known as solid waste management, which tries to improve and protect the health of dwellers and improve economic productivity and sustainability [1]. Constraints in raw material supplies, including critical metals (CMs) and rare earth elements (REEs), have been observed because of their increasing demand for green technologies, which forces society to think about solid waste management and material recycling. Recycling various wastes is a critical part of what we have come to know as the circular economy [2]. Over the last decade, the circular economy has received growing attention because of environmental benefits, resource conversation, and bringing materials back to the life cycle by creating a closed loop. Moreover, the circular economy should ultimately lead to helping overall economic growth [3]. In other words, the circular economy aims to decrease companies' and industries' reliance on the Earth's resources, which leads to saving a significant amount of energy and preventing the generation of gigatons of products that end up in landfills.

There are several methods to manage wastes based on the chemical and physical properties of the waste materials (e.g., organic versus inorganic, hazardous versus safe), and these have most often included storage in landfills and tailings ponds or treatment via solid waste incineration and other recycling processes [4–6]. Landfill mining and urban mining have become alternative methods to extract some of the valuable materials from wastes, like REEs that have been buried in the ground [7]. In urban mining, various

* **Corresponding author: Rafael M. Santos,** School of Engineering, University of Guelph, Guelph, Ontario N1G2W1, Canada, e-mail: santosr@uoguelph.ca
Nneka Joyce Odimba, Reza Khalidy: School of Engineering, University of Guelph, Guelph, Ontario N1G2W1, Canada
Reza Bakhshoodeh: Department of Civil, Environmental and Mining Engineering, The University of Western Australia, Perth, Western Australia 6009, Australia

CMs and REEs have been obtained and recycled from various end-of-life products and industrial wastes like electrical and electronic equipment waste, combustion residues, construction and demolition waste, exhausted oils, sewage sludge, previously landfilled wastes, and industrial wastes [8,9]. A significant amount of REEs can be recovered and recycled from consumer end-of-life products. Figure 1 shows the recoverable REEs from different end-of-life products. Yet, only about 18% of the total produced e-wastes (50 million tons of WEEE/year) has been recycled, and the rest has been disposed of into landfills or incinerated [10,11].

Although in the long-term landfill and urban mining for REEs will be able to supply a large portion of the global demand for raw REEs for manufacturing, in the near- to medium-term mining will still dominate this supply. However, the primary mining of REEs is geopolitically dominated by a few countries, e.g., China and Russia hold 53% of global total rare earth oxides plus yttrium oxide (TREO + Y) [12]. Hence, secondary mining of REEs from mine tailings resources could expand REE supply to a wider range of geopolitical regions, especially mining-active economies such as Canada, Australia, Brazil, Chile, and South Africa. Carbonatites, igneous rocks made up of REE-carbonate minerals associated with silicates and other minerals, presently represent the primary source of REE mining [13], and heavy REEs (HREEs) are primarily speciated as carbonates in other rocks such as weathered granite [14]. Recent research has been conducted to assess the potential of recovering REEs from carbonatite-rich mine tailings in Canada and South Africa. Edahbi et al. [15] identified Gd and Yb (at <0.4 wt%) as the main HREEs in waste rocks from a carbonatite deposit in Quebec, Canada. Gómez-Arias et al. [16] identified diopside (pyroxene), phlogopite (mica), and microcline (feldspar) as the main silicate minerals associated carbonates in carbonatite from the Phalaborwa (Palabora) Complex in South Africa.

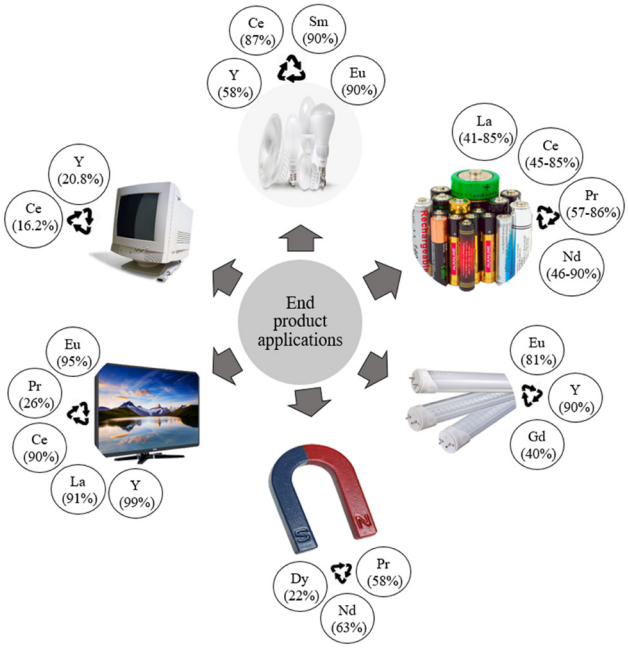

Figure 1: Recoverable REEs as % (w/w) in end-of-life products.

Recovery of REEs from waste materials can be done by chemical extractions via either pyrometallurgical or hydrometallurgical routes [17]. In the pyrometallurgical method, solid waste is smelted after mixing with metal concentrates for metal recovery, which consumes a large amount of energy and produces secondary wastes. In the hydrometallurgy method, large quantities of chemical agents (acids) have been used to solubilize metals, which have a high operational cost and can have negative environmental impacts. Therefore, the applications of environmental biotechnology and bio-hydrometallurgical process have been defined to improve efficiency, operating cost, and energy consumption [18].

It is challenging, and often not possible, to accurately study the behavior of experimental waste treatment and conversion systems, because of the level of chemical, physical, and biological complexity of these systems, and the varying scales of time involved (certain processes occur in the order of seconds or minutes, while others take years or decades). To overcome these challenges of experimental systems, geochemical models can be used to predict and interpret the geochemical processes that take place over different time scales [19]. As a popular tool, the geochemical equilibrium model is used to predict the phases and speciation of elements and the saturation index of minerals in solutions at equilibrium. The geochemical computer software commonly used in environmental, geological, and other hydrometallurgical studies include Visual MINTEQ, PHREEQC, and The Geochemist's Workbench (GWB). Examples of the use of geochemical models include the optimization of environmental remediation processes, the identification of the parameters that govern processes in groundwater systems, and the design of techniques to prevent the release and transport of contaminants from waste storage sites to ground and surface waters [20]. Although modeling and computer simulation are not substitutes for experimental work, they are valuable for bridging the knowledge gaps that always exist between laboratory experiments and field phenomena and between processes that occur within short time scales and are experimentally observed and processes that will occur over longer time scales and cannot be predicted experimentally.

To this end, this work investigates and discusses the geochemical behavior and speciation of two critical HREEs, europium (Eu) and ytterbium (Yb), which may be associated with rocks containing one of four silicate minerals (chrysotile ($Mg_3Si_2O_5(OH)_4$), forsterite (Mg_2SiO_4), Mg-montmorillonite ($Mg_{0.495}Al_{1.67}Si_4O_{10}(OH)_2$), and phlogopite ($KAlMg_3Si_3O_{10}(OH)_2$)), in a simulated (bio)hydrometallurgical system intended to recover REEs from mine tailings. The study aimed at investigating the congruent or incongruent (i.e., sequential) dissolution of silicates and oxides, and as such the pH at which one or both mineral phases dissolve, and to also assess the formation of transient mineral phases. The motivation was to determine if a (bio)hydrometallurgical process should aim to fully dissolve all minerals for subsequent selective recovery of the REEs, or if the REE oxides/carbonates/hydroxides can be recovered as enriched solids after the partial or total dissolution of the silicate matrix minerals, thus recoverable by physical separation means.

2 Background literature

2.1 REEs

Rare earth metals are extensively useful for a wide range of applications in different industrial sectors such as petroleum, metallurgy, nuclear energy, textiles, etc. They have also become an indispensable and important resource in several high-tech companies for the production of several modern devices such as mobile phones, computers, solar cells, wind turbines, televisions, hybrid cars, fluorescent lights as well as biomedical applications [21–23]. Hence, there is an ever-increasing demand for REEs in correspondence to the increasing demand for industrial production and the rapid evolution of the technological market. The required functionality of different REEs and the possibility of their broad use are predetermined by the combination of their unique chemical and physical properties [24]. They can be used in two major directions (Figure 2). In some cases, a single REE is required such as the use of La in the production of nickel hydride batteries while other applications require the use of non-separated REEs, i.e., a mixture of REEs, such as the use of Eu, and Y for rare earth phosphors used in the production of fluorescent lights [22].

REEs mostly fall into two groups with varying levels of use and demand. They can either be classified under light rare earths (LREE) or HREE. These classifications are based on their atomic numbers. LREEs include lanthanum (La), cerium (Ce), praseodymium (Pr), neodymium (Nd), and samarium (Sm) and HREEs include europium (Eu), gadolinium (Gd), terbium (Tb), dysprosium (Dy), holmium (Ho), erbium (Er), thulium (Tm), ytterbium (Yb), lutetium (Lu), and yttrium (Y), which are less common and more valuable [21].

The abundance and ease of accessibility of REEs is a major concern to the industrial sectors as the primary sources of these metals are becoming insufficient to meet the high demands as the concentrations of these metals are focalized in limited areas. Also, high energy-intensive processes are involved in the extraction of these REEs from their primary ores [25]. This is why a lot of manufacturing and technologically inclined countries are on the lookout for alternative sources of REEs [21].

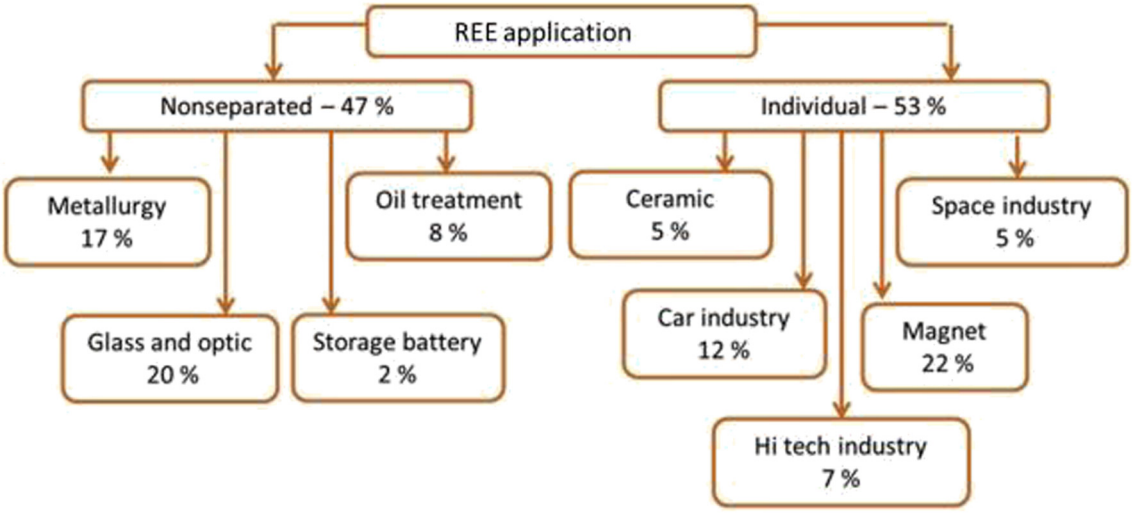

Figure 2: Different industrial applications of REEs (individual and mixture of REEs) [24]. Copyright © 2020; Elsevier (5505521280816).

Amongst these REEs, four of them namely lanthanum, yttrium, neodymium, and cerium, constitute over 85% of the world's production. Even though the recovery of these metals from their ores is quite challenging, it is still very possible to carry out [26]. However, the recovery of other REEs which are usually used in much smaller quantities, especially the ones in the HREE category, is more difficult as a result of the technical challenge connected to the separation of these REEs from their sources. The use of acid leaching has gained popularity in the recovery of these metals. Studies have shown that lowering the pH of the extraction system promotes the dissociation of the REEs from their ores.

2.2 Industrial wastes generated containing REEs

The automotive industry is one of the biggest industries in modern life because of its indispensability. The total global number of automobile owners in 2010 exceeded 1.1 billion. From this amount, the USA and EU have accounted for about 50% comprising 240 million and 270 million units, respectively [27]. All of these vehicles will be considered wastes after their end of life. For example, based on available reports, the number of end-of-life vehicles will be about 1.86 billion short tons in 2030 [28]. Therefore, the processing and recycling of this type of waste, which contains REEs (especially Dy), are significant. Hoenderdaal et al. [29] reported that electric vehicles accounted for about 23% of the worldwide demand for Dy. The main REE application in electric vehicles is batteries. Based on Alonso et al. [30], the main REE applications in electric vehicles are the nickel-metal hydride battery (about 3.5 kg) and then the generator and driving motor (about 0.6 kg) [30]. Figure 3 shows the distribution and the REE mass concentration for an electric and conventional car.

Coal mining wastes and combustion residuals (coal fly ash [CFA]) have been gaining attention as attractive alternative resources for REEs [31–33]. The current

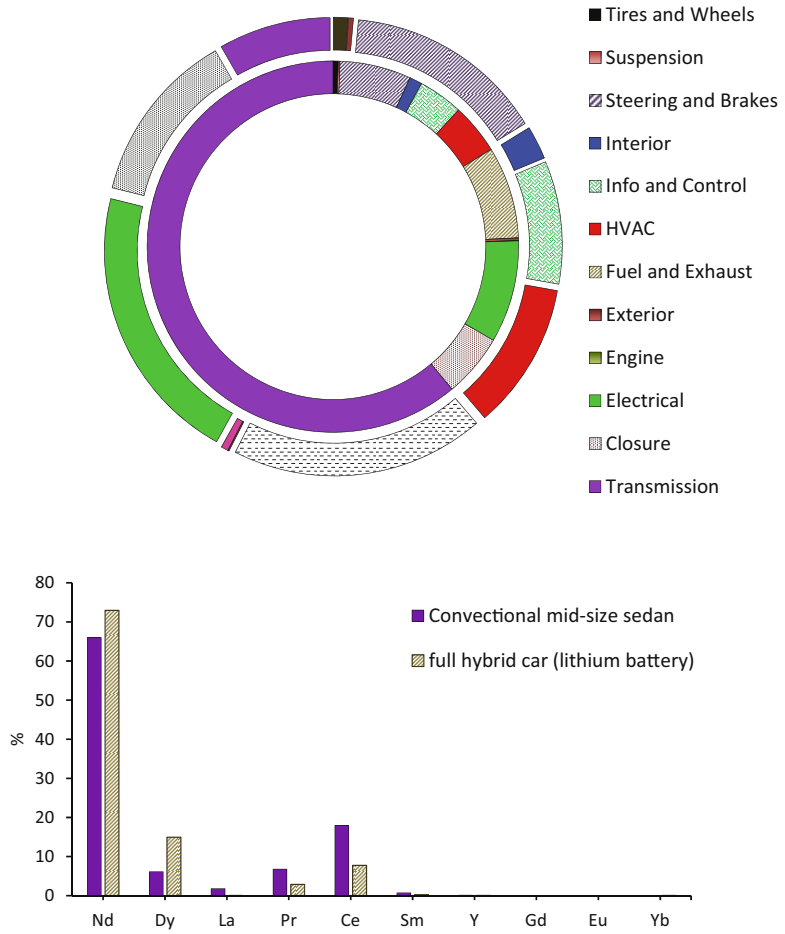

Figure 3: (Top) REE distribution of a hybrid car with a lithium battery (inner pie chart) and conventional car (outer pie chart); (bottom) REEs in an electric and conventional car.

disposal practices used have been considered as not being environmentally friendly due to the toxicity, leachability, and radioactivity of these residues which result in environmental pollution [34]. Hence, the reuse and possible detoxification of CFA have led to their discovery as alternative sources of REEs. These alternative sources are worthy of exploitation as it has been reported that 36 million short tons of fly ash are generated annually in the US alone [32]. The recovery of REEs from coal-related materials has been reported to be advantageous over their recovery from other commercial sources for a few reasons. First, Vass et al. [35] noted that coal-related materials contain lower concentrations of radionuclide as compared to traditional ore deposits. Also, Honaker et al. [36] reported that they contain more of the HREEs and critical REEs (CREEs) than the LREEs. Furthermore, the cost of mining these REEs is relatively insignificant as they are generated as byproducts from the coal production and utilization processes [37]. Sarswat et al. [38] discussed how the mitigation of environmental issues is addressed by the recovery of these REEs from coal-based materials.

Red Mud is a bauxite residue produced from the production of alumina by the Bayer process. Its high alkalinity and difficulty to handle and dispose present an environmental challenge to all alumina-producing industries and regulating bodies [39,40]. It has been reported to be generated in the range of 1–1.5 tons for every 1 ton of alumina produced [41], as illustrated in Figure 4. Furthermore, this waste generation amounts to an even larger quantity on a global scale due to the increasing demand for alumina [42].

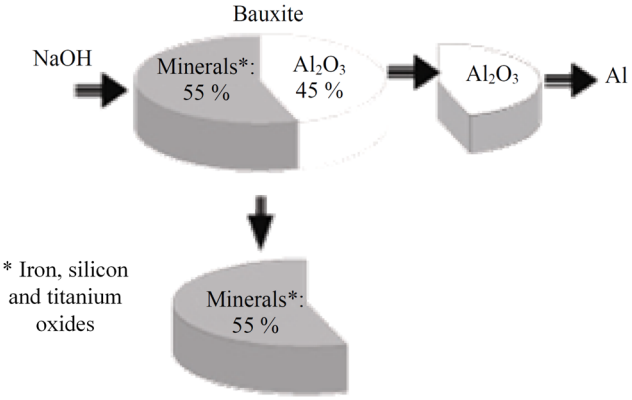

Figure 4: Components of bauxite consist of aluminum oxide that is dissolved during mining to produce aluminum, leaving behind the bauxite residue which contains various minerals [57]. CC-BY.

2.3 Conventional methods of REEs recovery from different industrial wastes

The use of direct acid leaching has gained popularity in the extraction of REEs from industrial wastes and complex ores. Strong acids such as hydrochloric acid, nitric acid, sulfuric acid, etc., have been tested for their ability to potentially recover REEs from CFA [43–46], and phosphoric acid has been suggested as more appropriate for phosphate ore to avoid the introduction of extra ion impurities [47]. If REEs are not fully oxidized before acid leaching, they can undergo oxidative roasting [48], or if the reduced REE is more susceptible to acid leaching, then it can be reduced with thiourea prior to leaching [9].

It has been noted that direct acid leaching of REEs is challenging and inefficient when they are attached to the predominant glass phase of the CFA particles, thus making it difficult for them to erode [49]. Wen et al. [31] noted that HCl achieved the highest leaching efficiency of 71%. Hence, the preconcentration of REEs using physical separation methods before leaching has been recommended [50,51].

Fractionation of CFA particles is usually done based on their contrasting physical characteristics which include magnetism, particle size, density, etc., and this fractionation has been proven to be an important step because REE extraction from certain fractions is more enriched in REEs, thus making their overall recovery more economically viable [37]. Three reasons have been suggested as valid explanations for the use of physical separation methods. First, REEs are preferentially associated with the glass phase in fly ash, which are usually found in finer fractions than in coarse fractions [52]. Second, extremely small particles made up of REEs associated with organic matter tend to augment the finer fractions of fly ash [49]. Finally, these organic-bound REEs partially volatilize and are deposited on the fine particles of fly ash [53].

Different separation methods have been employed for partitioning CFA particles into different fractions. These methods are magnetic separation [51,53,54], gravity and flotation separations [23], and microwave irradiation [55,56]. From the results obtained from the different separation methods used, it can be concluded that these methods help to pre-concentrate REEs from coal combustion ash. Hence, a high-grade material that serves as feed material for subsequent downstream processes (which includes acid leaching) is delivered, which leads to a reduction in the overall recovery cost.

2.4 Bioleaching of REEs

The solubilization of metals from their ores is based on three mechanisms, namely: acidolysis, complexolysis,

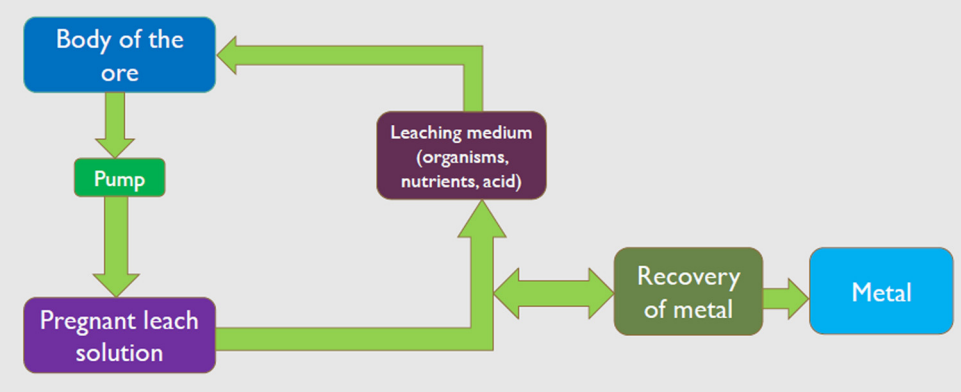

Figure 5: Process flow of a typical bioleaching process of heavy metals.

and redoxolysis [58]. The microorganisms obtain their energy through the oxidation of iron(II) and reduced sulfur compounds, with oxygen serving as the electron acceptor in these reactions. The overall bioleaching reaction (Eqs. 1–3) shows that 3.5 moles of oxygen are required to oxidize 1 mole of pyrite [59].

$$2FeS_2 + 4H + 7O_2 + 2H_2O \rightarrow 2Fe^{2+} + 4H_2SO_4 \quad (1)$$

$$2Fe^{2+} + \frac{1}{2}O_2 + 2H^+ \rightarrow 2Fe^{3+} + H_2O \quad (2)$$

$$2Fe^{3+} + Cu^0 \rightarrow 2Fe^{2+} + Cu^{2+} \quad (3)$$

Typically, the leaching medium which contains the carbon source, the microorganisms, and the produced metabolites (organic acids, chelating agents, amines, etc.) is applied to the metal ore and the process is monitored and evaluated sequentially for the dissolved metals in the leachate as illustrated in Figure 5. Operating conditions of the bioleaching process include [60]: (i) an adequate supply of oxygen is a prerequisite [61]; (ii) pH values less than 5 are a necessary condition for microbial leaching [62];

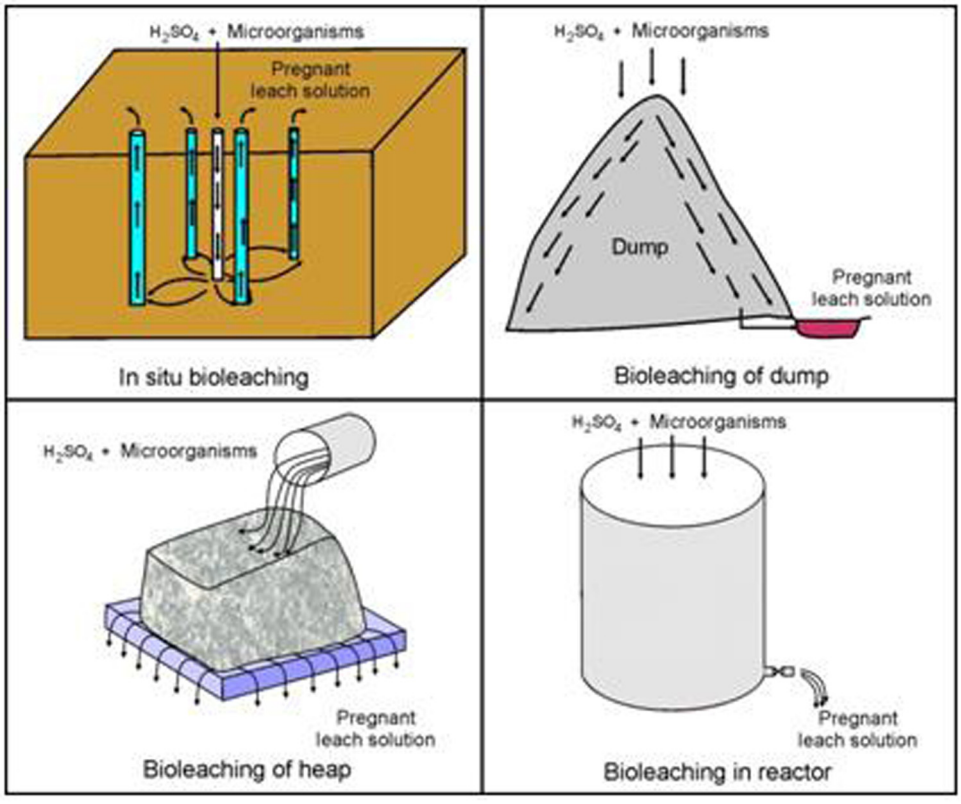

Figure 6: Different techniques of bioleaching currently used in the recovery of heavy metals [63]. CC-BY-NC.

(iii) optimum temperatures of 28–30°C are required for mesophilic organisms while higher temperatures equal to/greater than 50°C are required for thermophilic organisms for leaching [64]; (iv) high tolerance to heavy metals and various strains may even tolerate 50 g·L^{-1} Ni, 55 g·L^{-1} Cu, or 112 g·L^{-1} Zn; the leaching of metal sulfides is accompanied by an increase in metal concentration in the leachate [65]; (v) availability of the substrate; the ideal condition exists when the substrate is soluble such as with ferrous sulfate. For insoluble substrates, another requirement is adequate exposure to the sulfide minerals [65]; and (vi) particle size of 42 µm is regarded as the optimum for efficient bioleaching activity [66]; a decrease in the particle size means an increase in the total particle surface area so that higher yields of metal can be obtained without a change in the total mass of the particles.

As illustrated in Figure 6, bioleaching techniques can be classified into four domains, which are summarized as follows.

2.4.1 *In situ* bioleaching

According to Pradhan et al. [67], this method is used with abandoned and underground mines where conventional mining of the metal ores cannot occur as a result of small deposits left in the mines. Pipes are inserted into the mine pit to apply aeration and also to bring out the leachate under high pressure.

2.4.2 Dump bioleaching

The low-grade ore is leached at their place of disposal [67]. The leaching medium is applied to the dump using sprinklers. The solution is then allowed to flow down the dump and penetrates through the dump. The microorganisms use this solution to increase population, enough to catalyze the mineral oxidation leading to the dissolution of the metals into the leachate. This process is

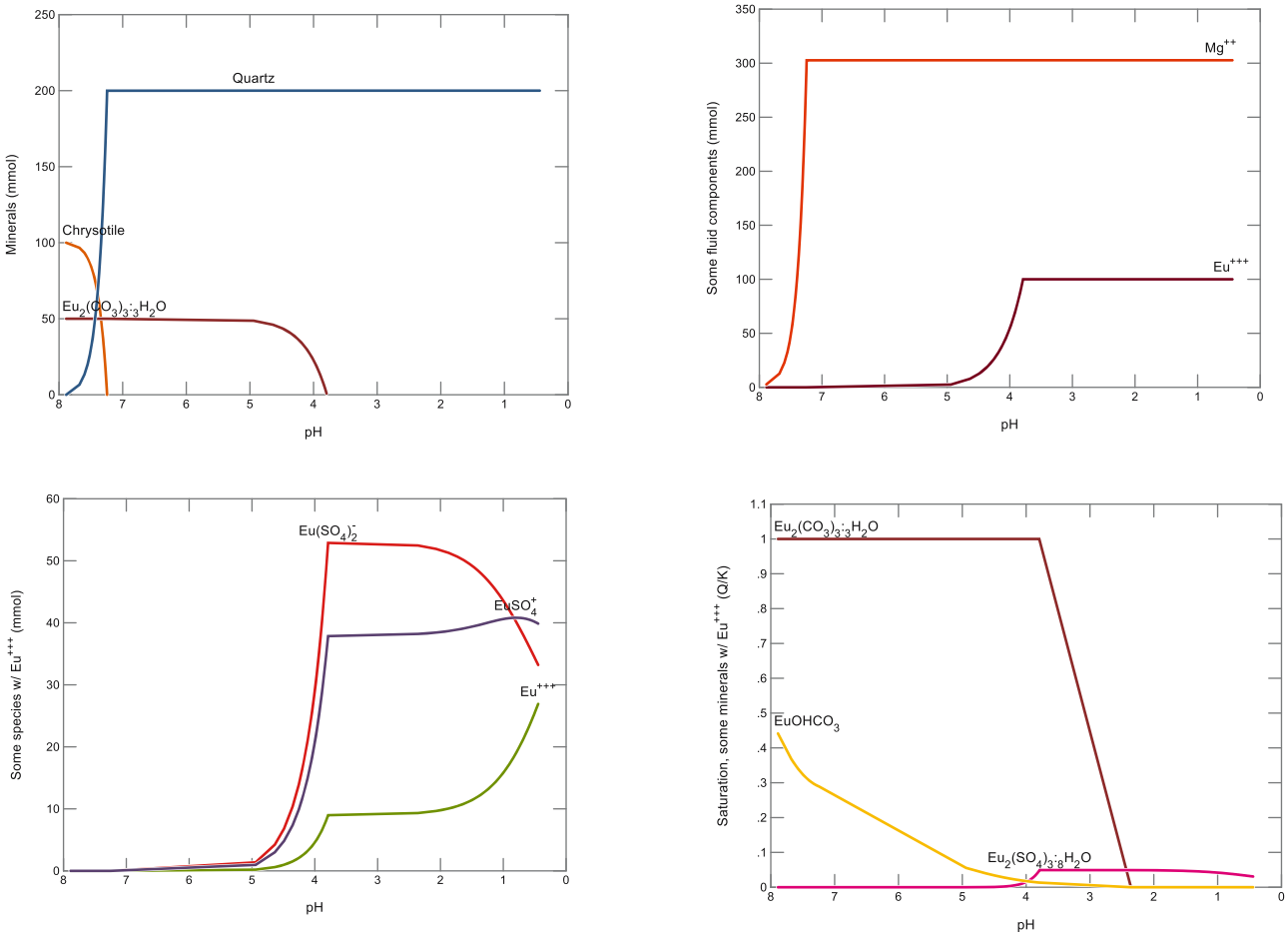

Figure 7: Geochemical modeling of chrysotile with $Eu_2(CO_3)_3{:}3H_2O$ using H_2SO_4 as the reactant.

however time-consuming and the complete dissolution of the metals is difficult due to the large particle size and the different rates of percolation of the leaching solution.

2.4.3 Heap bioleaching

This process is similar to dump bioleaching. It involves the application of a leaching solution containing the microorganisms and acids on low-grade ores heaped into large piles [68]. The microorganisms attach to the ore particles as the solution infiltrates into the heaped ores from the top. To maintain the aerobic state of the process, the air is injected into the heap through already laid pipes. The metals dissolve into the solution which is then collected for further extraction.

2.4.4 Stirred tank reactor bioleaching

This involves the use of reactors that are usually highly aerated. The ores and leaching solution are put into the tank which has a stirrer that is used for mechanical agitation. This agitation enhances the leaching and dissolution of the metals into the solution, which is collected at a designated outlet of the tank. The leaching process occurs in continuous-flow reactors placed in series. This method allows for better process control as compared to the other forms of bioleaching [63].

Various factors exert rate-limiting effects on the bioleaching process [69]; a few of these factors are highlighted as follows:

- The mass transfer of oxygen, carbon dioxide, and nutrients can limit the reaction.
- An increase in oxygen supply can lead to a higher concentration of dissolved oxygen (DO). DO concentration of above 5 ppm can exert an inhibitory effect on the bioleaching process [59].
- The formation of biofilms during leaching can impede microbial activities hence causing a reduction in the rate of bioleaching.
- A decrease in the particle size and shape means an increase in the total particle surface area leading to a higher yield of metal.

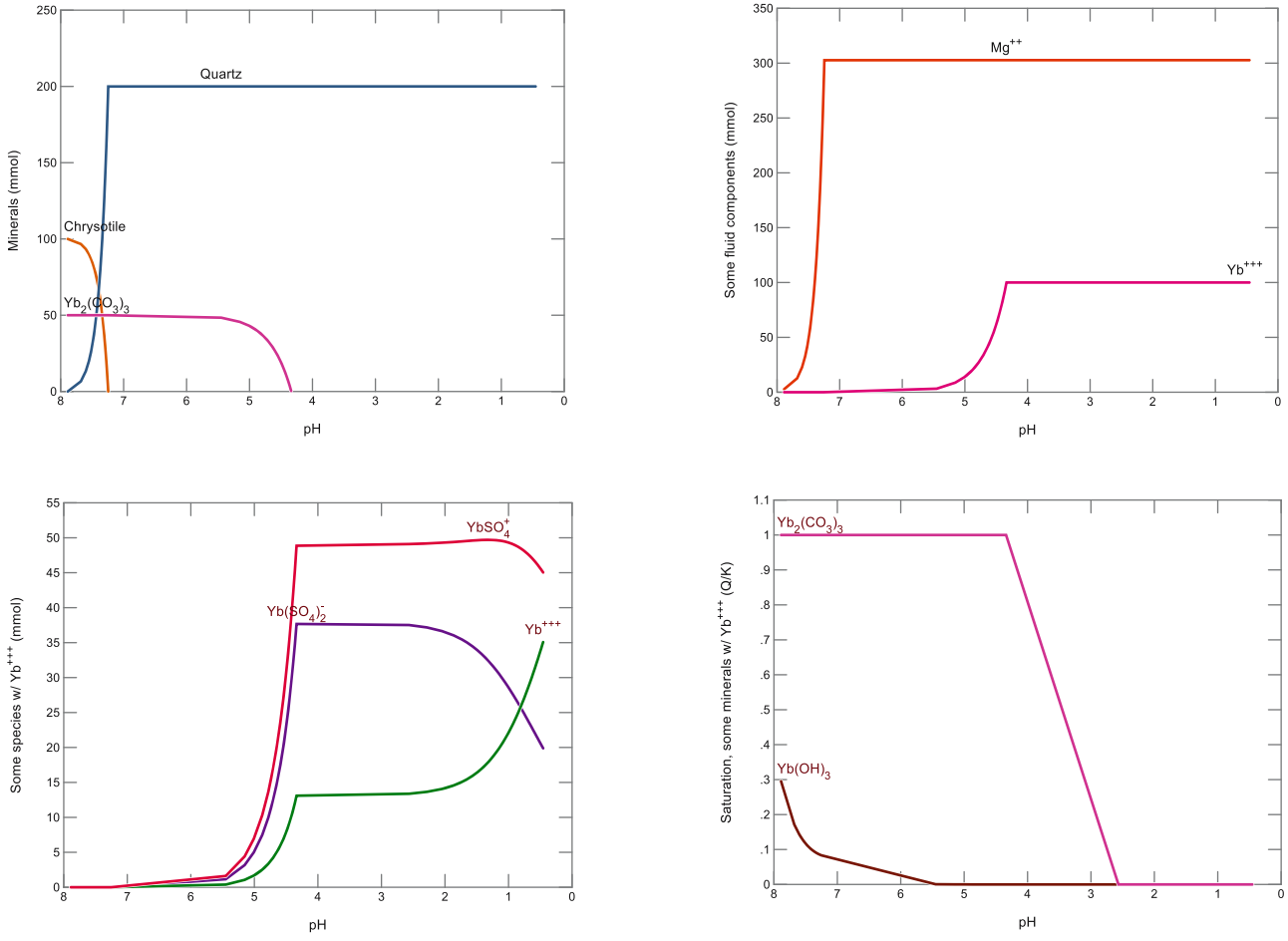

Figure 8: Geochemical modeling of chrysotile with $Yb_2(CO_3)_3$ using H_2SO_4 as the reactant.

- The pH of the reaction can significantly impede the rate of bioleaching. As earlier discussed, bioleaching occurs under acidic conditions; therefore, pH greater than 5 can reduce metal dissolution.
- Temperature is also an important rate-limiting factor. The extreme temperature that may be commonly associated with dump and heap bioleaching can affect the cell wall components of the microorganisms and cause denaturing of enzymes and other biological components of the organisms.
- While geochemical modeling assumes that all minerals are in perfect contact with the solution, it might not represent the real conditions, and this can be investigated through experimental work. For example, the bioproducts of the system could cause mass transfer inhibition (shrinking core) and passivation of bioleaching [70]. This could hinder contact of microorganisms and leaching media and hence interfere with the leaching process.
- The geochemical modeling assumes that minerals are pure, while they might contain trace amounts of heavy metals (and these trace amounts may dissolve during the leaching process). There are a few studies that have exclusively focused on heavy metal extraction through bioleaching [71].

3 Methodology

The modeling investigation of the leaching of two different HREEs, europium and ytterbium carbonates, from four different silicate minerals, namely chrysotile ($Mg_3Si_2O_5(OH)_4$), forsterite (Mg_2SiO_4), Mg-montmorillonite ($Mg_{0.495}Al_{1.67}Si_4O_{10}(OH)_2$), and phlogopite ($KAlMg_3Si_3O_{10}(OH)_2$), were conducted in the GWB v15.0. The minerals were selected to include one representative from each of the main groups of hydrated phyllosilicates (chrysotile from the serpentine group, montmorillonite from the clay minerals group, and phlogopite from the mica group), plus forsterite as the anhydrous orthosilicate. One reason to choose these two specific REE carbonates

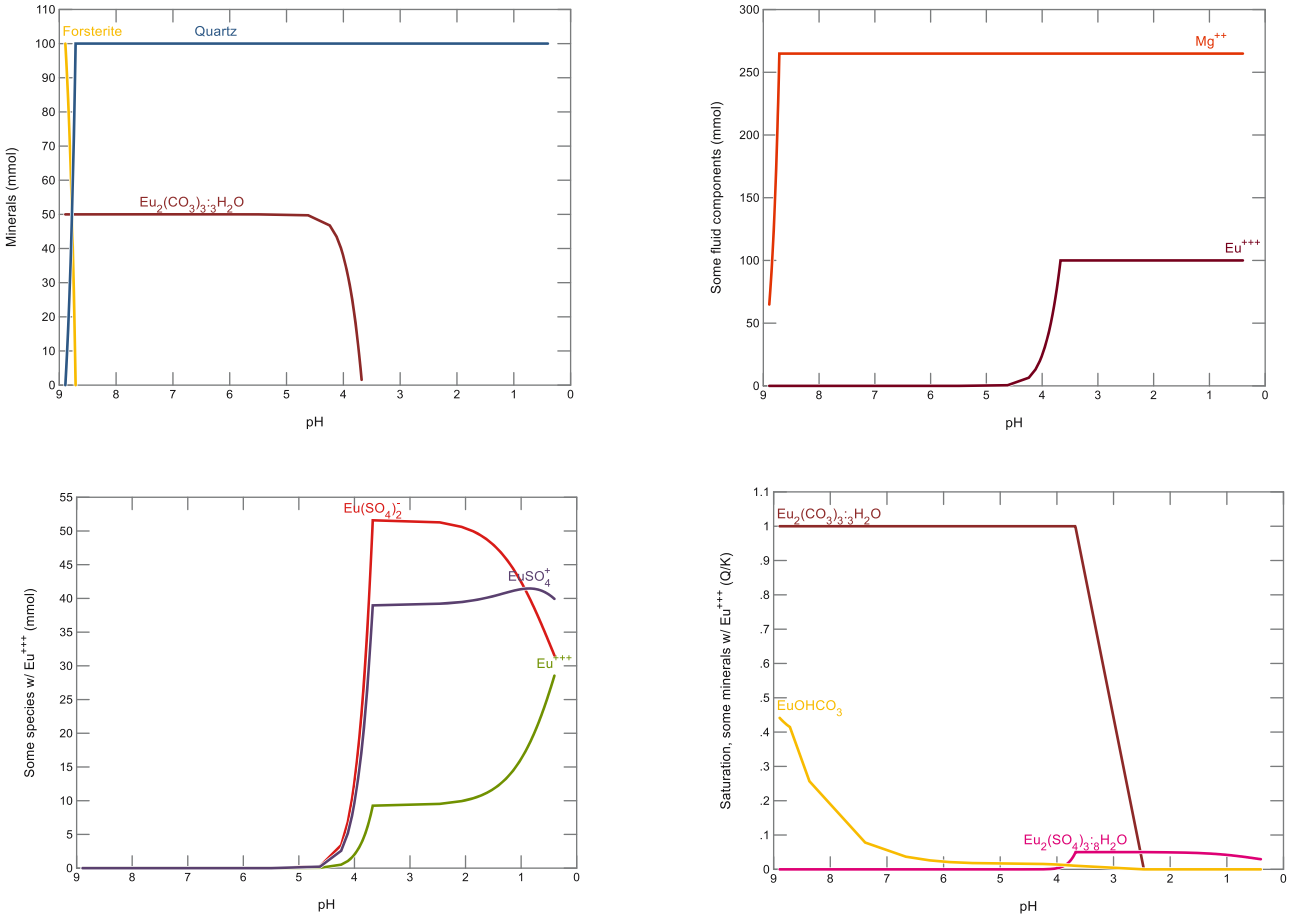

Figure 9: Geochemical modeling of forsterite with $Eu_2(CO_3)_3{:}3H_2O$ using H_2SO_4 as the reactant.

was that the thermodynamic databases did not include data for many REE carbonates. The aim was to study a diversity of silicates that may be present in association with carbonatite tailings. The leaching study was done using H_2SO_4 and HCl as the inorganic acids and lactic acid ($CH_3CH(OH)COOH$, produced from lactobacillales – lactic acid bacteria) as the organic acid, to compare the extent of the reaction and the behavior of the REEs subjected to these different acids in a simulated reaction.

Each simulation starts with the equilibration of silicate minerals and oxides of Eu and Yb ($Eu_2(CO_3)_3{:}3H_2O$ and $Yb_2(CO_3)_3$) with an aqueous solution of dilute salts exposed to air, followed by the addition of inorganic (H_2SO_4 and HCl) and organic (lactic) acids to this system to simulate chemical leaching and chemoorganotrophic bioleaching conditions [58], respectively. The following paragraphs, and the Supplementary Material, detail the precise methodologies for constructing and running these models.

First, on the basis pane (Figure S1), Mg^{++} was swapped for the minerals of interest, i.e., chrysotile, while $Eu_2(CO_3)_3{:}3H_2O$ was swapped in place of Eu^{+++}. Two gases (O_2(g) and CO_2(g)) were added at atmospheric concentrations, and other minor cations and anions (Na^+, Cl^-, and SO_4^{2-}) were added to charge-balance the reaction under room temperature of 25°C, as shown in Figure S1. On the reactant pane (not shown), 100 mmol of chrysotile and 50 mmol of $Eu_2(CO_3)_3{:}3H_2O$ were added to run the reaction. This reaction equilibrates the dilute aqueous solution with the two rock minerals (one silicate and one carbonate), leading to the solution coming into equilibrium with the rock. Since other silicate minerals are thermodynamically more stable than chrysotile but are not expected to form due to kinetic limitations, all other possible Mg minerals were "suppressed" except for chrysotile. After this first reaction was run, the entire system was "picked up" to turn the equilibrated condition into the initial condition for the next reaction step, as shown in Figure S2. In this second reaction step, where acid leaching is simulated, either H^+ and SO_4^{2-} were added to the reactant pane (not shown) at a ratio of 2:1 (to simulate inorganic acid leaching) or H^+ and $C_2H_5O(COO)^-$ (lactate) were added to the reactant pane at a ratio of 1:1 (to simulate organic acid leaching). In organic acid leaching

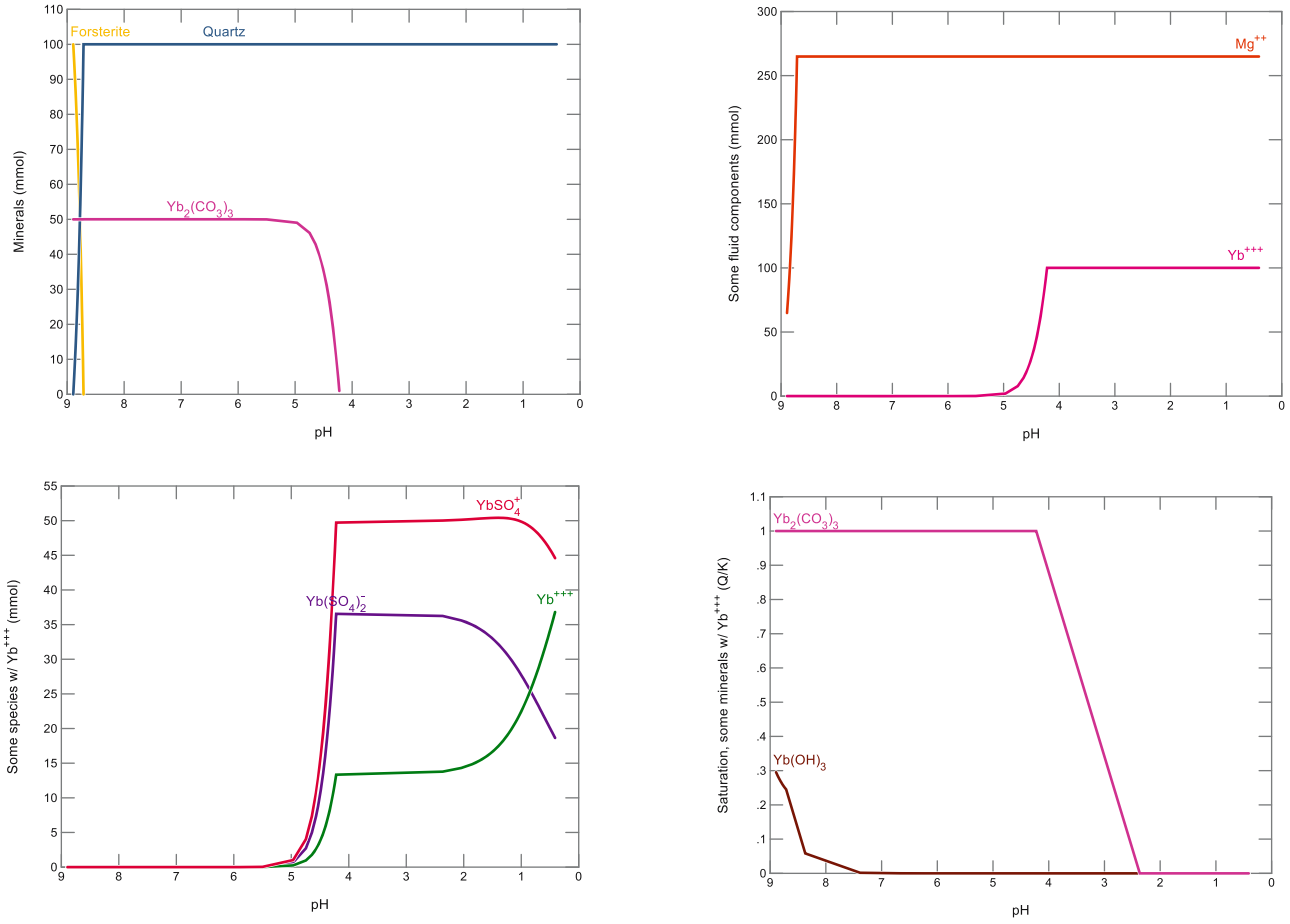

Figure 10: Geochemical modeling of forsterite with $Yb_2(CO_3)_3$ using H_2SO_4 as the reactant.

models where hydrochloric acid was added as a co-lixiviant, H^+ and Cl^- were also added to the reactant pane at a ratio of 1:1. It should be noted that GWB treats reactants as titrants, so the leaching reaction results are obtained as a function of acid addition amount, from the initial equilibrated pH to a final acidic pH. Following these steps, the leaching model was run, and the results were produced and analyzed for different behavior patterns such as the dissolution and precipitation of minerals, the mineral saturation, the components of Eu in fluid, and the speciation of Eu.

The same processes described above were repeated for forsterite, except that Mg^{++} was swapped for forsterite in the basis, as shown in Figure S3a. Similarly, for the leaching of Yb, the only difference compared to the above is that $Yb_2(CO_3)_3$ was swapped for Yb^{+++} on the basis pane, as shown in Figures S4a and S5a for chrysotile and forsterite, respectively. There was a slight difference, compared to the above, in the modeling of montmorillonite and phlogopite. As Al^{3+} is present in these minerals, it was essential to include this in the basis pane for the model to run. Hence for the modeling of these two minerals, on the basis pane, Mg^{++} was swapped for magnesite ($MgCO_3$), while Al^{+++} was swapped for the mineral of interest, i.e., montmorillonite or phlogopite. In addition, in the suppression steps, all Mg and Al minerals, except for the minerals of interest and for gibbsite ($Al(OH)_3$), which is a product of the reaction), were suppressed. The remaining aspects of these models were the same as described above. Figures S6–S10 show the basis of these models for the two reaction steps: water equilibration (Figures S6, S8a, S9a, and S10a) and acid leaching (Figures S7, S8b, S9b, and S10b). Following these steps, the results were analyzed as aforementioned.

The second part of Supplementary material (Figures S11–S18) contains the raw model outputs for the simulation scenarios aforementioned, which were used to generate graphs presented in Section 4.

4 Results and discussion

The results of this chapter are presented and discussed in two parts, and the list of figures contains the relevant

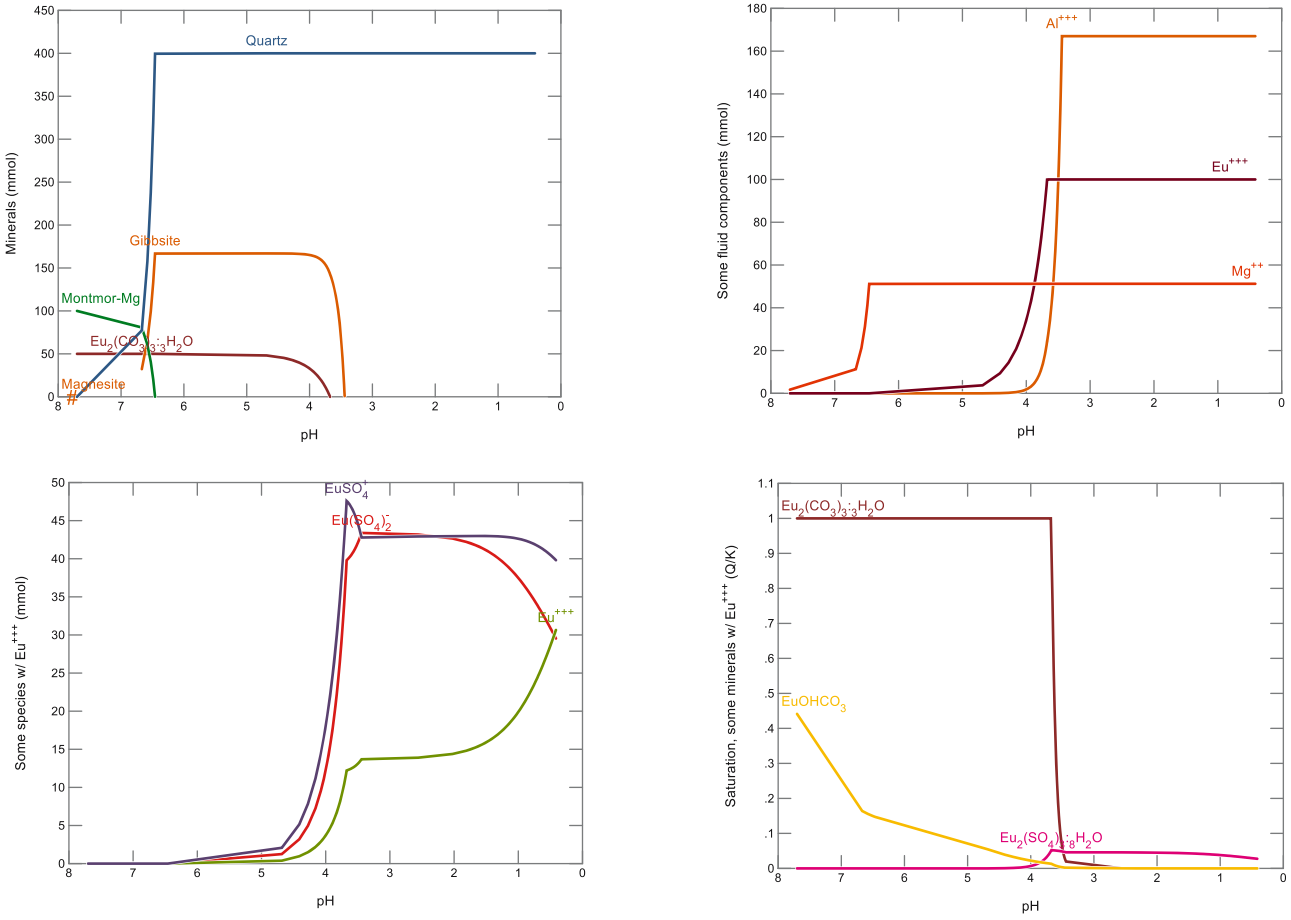

Figure 11: Geochemical modeling of montmorillonite with $Eu_2(CO_3)_3{:}3H_2O$ using H_2SO_4 as the reactant.

graphs. Section 4.1 presents the geochemical modeling results of Eu and Yb from four silicate minerals (chrysotile, forsterite, montmorillonite, and phlogopite) using sulfuric acid as the inorganic acid. Section 4.2 presents the geochemical modeling results of the same two REEs leaching from the same four silicate minerals, but using lactic acid as the organic acid, with and without hydrochloric acid. From these results, it is possible to assess the extent of silicate and REE leaching as a function of the amount of lixiviant added, and in turn as a function of solution pH. It is also possible to observe if the leaching of the two initial mineral components occurs concurrently or sequentially, and if any intermediate mineral phase that is both thermodynamically favorable and also kinetically likely, forms.

4.1 Geochemical modeling of REEs leaching from silicate minerals by inorganic acid

The first step of the modeling was to equilibrate the silicate mineral and REE of interest with a dilute salt solution, before leaching commencing in the second step of modeling. The results of geochemical modeling (the trend of mineral dissolution/the fluid component of system/speciation of REEs and saturation index of minerals over a range of pH) for leaching of chrysotile, forsterite, montmorillonite, and phlogopite with H_2SO_4 are depicted in Figures 7–14. Looking at these figures, which present the pH-dependent data of the leaching step of the modeling, it is possible to observe that the initial pH values of these systems were in large part similar, around a value of 8, with one significant exception for forsterite. In the forsterite system, the initial pH was close to 9, and this is explained by forsterite being a more reactive, and hence less insoluble silicate mineral, compared to the other three (chrysotile is a hydrated monoclinic silicate of the serpentine group, while montmorillonite and phlogopite are smectite and mica clays, respectively).

Inorganic acids are characteristically strong acids, particularly H_2SO_4. This means that as more acid is added to a solution, the lower the pH becomes. Minerals can, however, act as buffering agents, consuming acidity as they dissolve. In this model, sufficient acid was added to

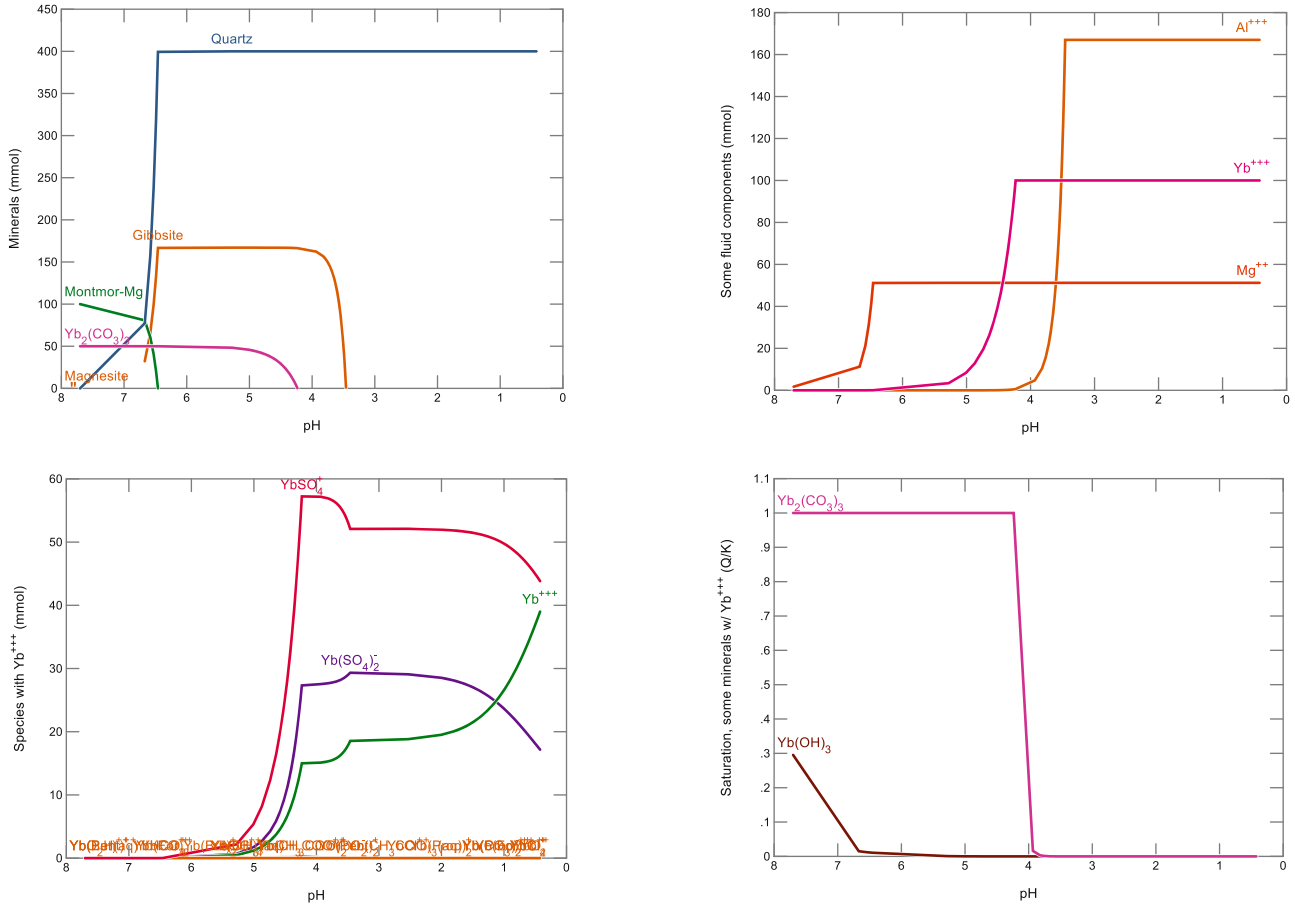

Figure 12: Geochemical modeling of montmorillonite with $Yb_2(CO_3)_3$ using H_2SO_4 as the reactant.

ensure that both the silicate mineral and the REE in the system fully dissolved. This is what is shown in the top left subfigures of Figures 7–14. In the first instance of these subfigures, it is observable that in all cases it is the silicate mineral that dissolves (i.e., leaches) first (silicate minerals tend to dissolve at higher pH values compared to REE carbonates). As aforementioned, the initial pH of these systems differed, and two more differences can be seen in the leaching of the silicate minerals. First, the "rate" of leaching (i.e., how suddenly the minerals dissolved with a reduction in pH) differed. Forsterite, being comparatively more reactive, leached over a very narrow pH range, while the other three silicates leached more gradually, over a pH range of around 0.5–1.5. Second, the pH value at which the silicate minerals had fully dissolved also varied. Forsterite was already fully dissolved at a pH value greater than 8.5, followed by chrysotile fully dissolving at a pH value just above 7, phlogopite leaching complete once the pH reached just below 7, and montmorillonite reaching the lowest pH of about 6.5 before fully dissolving. These trends further reaffirm that forsterite is the most reactive among the four silicates tested, and hence easier to leach, thus liberating the REE minerals contained within a silicate-rich rock. As expected, clay minerals are poorly reactive as these are relatively stable minerals (in geologic systems clay minerals are silicates that have weathered and hydrated, while forsterite is a mineral that is yet to weather), and hence required more acidity before they dissolved. Chrysolite fell in between, and it is a mineral that is known to be activated when it is dehydroxylated (calcinated at elevated temperature to remove chemically bonded water that stabilizes the silicate), so heat treatment of chrysotile-rich rock is a possible approach to help in liberating REEs contained within it.

Figures 7–14 show that one of the minerals to form after the dissolution of the silicates was quartz (SiO_2). This was the modeling result since other silicate minerals were not allowed to form in this leaching system, since it is kinetically unlikely that silicate minerals could rapidly form under the leaching conditions simulated (ambient conditions). Quartz is a stable mineral phase of SiO_2,

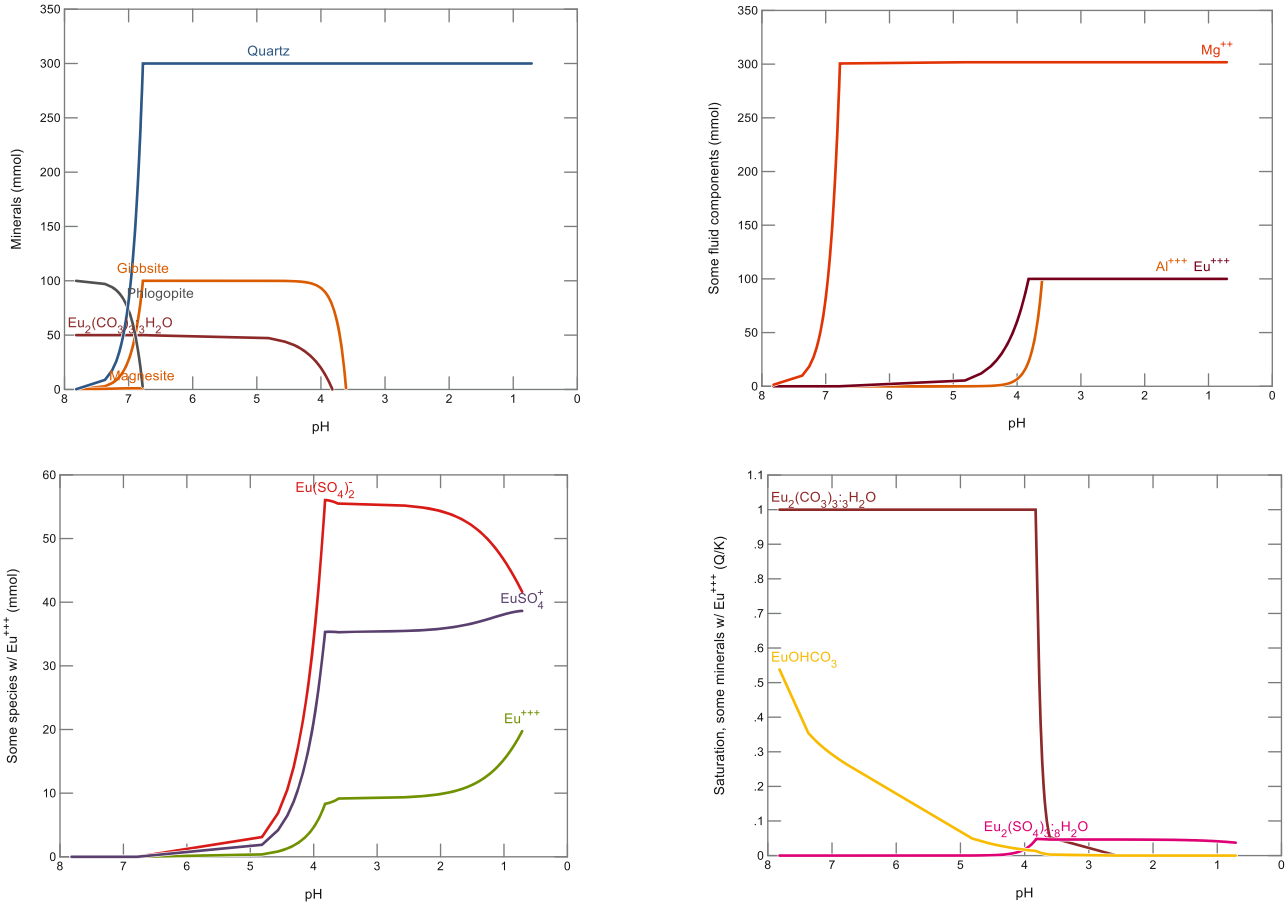

Figure 13: Geochemical modeling of phlogopite with $Eu_2(CO_3)_3{:}3H_2O$ using H_2SO_4 as the reactant.

which has low solubility. In reality, it is more likely that amorphous $SiO_{2(s)}$ would form, as quartz does take some time to crystallize, but amorphous silica was not a phase that was available in GWB. Quartz is expected to have a much lower density than carbonates of REEs (since Eu and Yb are heavy elements); hence, their separation can possibly be achieved via gravimetric methods (the densities of the mentioned minerals were checked in the GWB database). Two other intermediate and transient minerals were observed in the cases of montmorillonite and phlogopite leaching: magnesite ($MgCO_3$) and gibbsite ($Al(OH)_3$). In both cases, a small amount of magnesite formed in the early stages of leaching, and subsequently disappeared. Likely this is a result of the availability of Mg^{2+} (see top right subfigure of Figures 7–14) and CO_3^{2-} ions (not plotted) at near-neutral pH, inducing sufficient saturation of magnesite to lead to its precipitation. Oddly, this did not occur in the cases of forsterite and chrysotile, so more detailed analyses of the level of dissolved CO_2 in these systems could be done to understand what makes these systems undersaturated with respect to magnesium carbonates. Gibbsite, on the other hand, occurred and behaved similarly in both the montmorillonite and chrysotile systems. In these systems, it existed between pH values of roughly 3.5 and 6.5. Evidently, it only formed in these systems because these are the only two silicates that contain Al in their chemical composition. Also, aluminum is an amphoteric element, which means that it leaches at both high and low pH; hence, its solid (hydr) oxide form is only stable at moderate pH values, which is what is observed here. Gibbsite fully re-dissolved at a slightly more acidic pH in the case of montmorillonite, but these small differences can be attributed simply to slightly different aqueous compositions (and thus ionic strengths and activity coefficients) of the two systems.

In all cases, the REEs Eu and Yb started to leach in a lower pH value compared to their corresponding silicates in the system. This is a desirable outcome, as it means that physical recovery of grains of REEs can be attempted, for example via filtration or flotation process, once the leaching of the main silicates is completed. However, it is possible that REE-rich rocks also contain secondary mineral phases

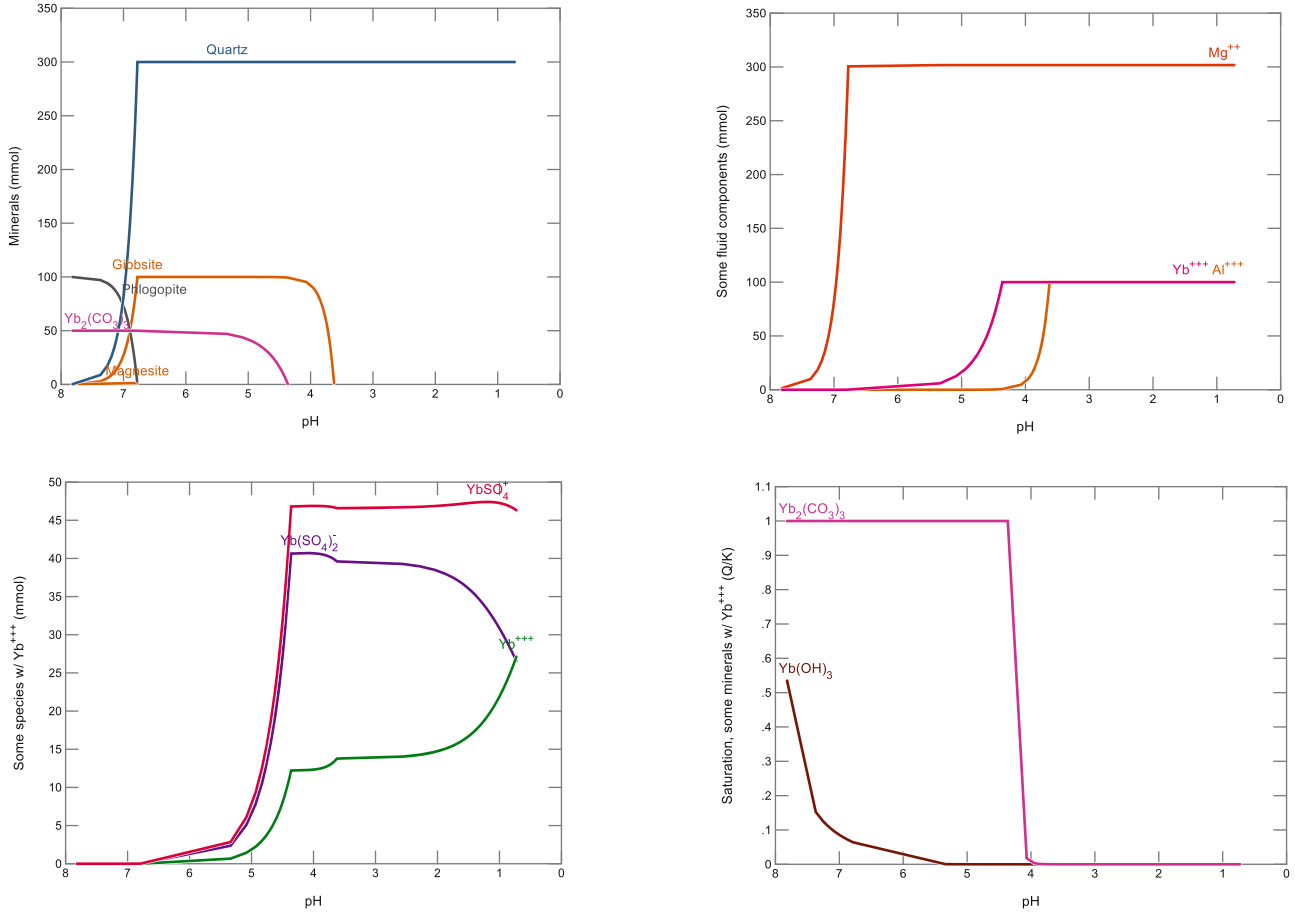

Figure 14: Geochemical modeling of phlogopite with $Yb_2(CO_3)_3$ using H_2SO_4 as the reactant.

that are more resistant to leaching than the studied silicates, so it is also of interest to know at which pH the REE carbonates are fully dissolved. Once fully dissolved, they could be retrieved from the solution via hydrometallurgical approaches such as selective precipitation, co-precipitation, ion-exchange, and electroplating. Bio-precipitation is also a possible approach, but not well-studied. Between the two REE carbonates, the Eu carbonate required more acidity to dissolve than the Yb carbonate. The former leached at around 3.5–3.9 in all systems, and the latter leached between approximately 4.1 and 4.5. Notably, in the two systems that had the intermediate mineral phase gibbsite, both REEs fully leached before the gibbsite started to leach. This is desirable to avoid co-leaching Al with the REEs, which could complicate REE recovery from the solution. In fact, it means that in these systems, the silicate can be first dissolved in a first leaching step at higher pH, then the residual solids containing the REE carbonate and the aluminum hydroxide are recovered and sent to a second leaching step at lower pH where the REEs can be dissolved, leaving the Al in the residual solid phase.

The bottom two subfigures in Figures 7–14 are shown to provide information about the speciation of the REEs once they enter the solution, and also the saturation states of other possible REE solid phases that could be present or form as intermediates. Interestingly, Eu predominantly speciates as an anion complexed to two sulfate ions, while Yb predominantly speciates as a cation complex to one sulfate ion. However, in both cases, the opposite ionic species (cation or anion) is also present in significant amounts. This may suggest that ion exchange is a complex process to use to fully recover dissolved REEs. Instead, it might be possible to use a solvent exchange, where the REEs are removed from the solution complexed to organic ligands. As for saturation states, in all cases, the secondary mineral phases of Eu and Yb are undersaturated at the pH values of interest (i.e., when separation would occur), and so there is little chance for the REEs to form intermediate minerals that can complicate separation.

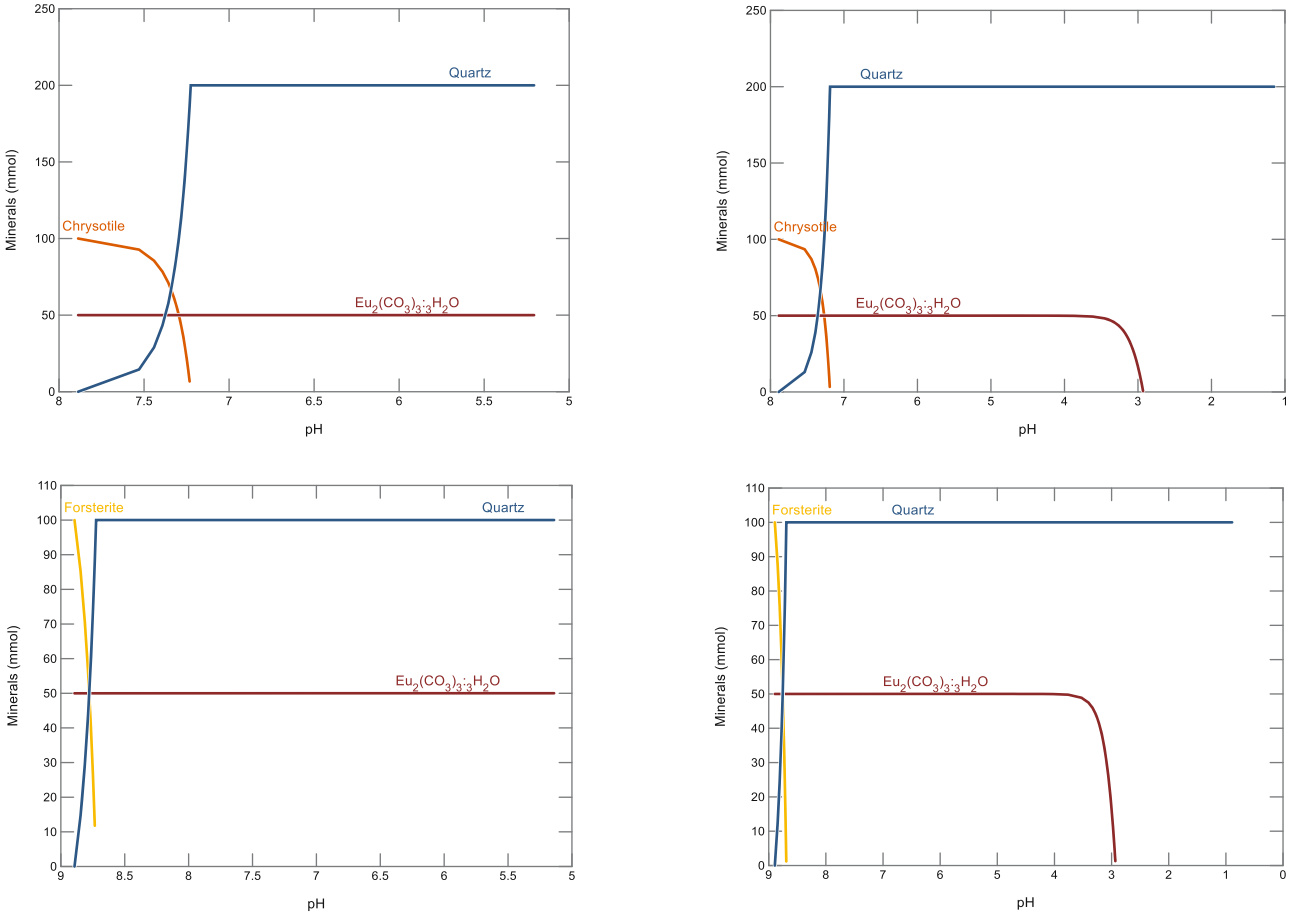

Figure 15: Modeling of (top) chrysotile with Eu using (left) lactate (right) HCl + lactate as reactants; (bottom) forsterite with Eu using (left) lactate (right) HCl + lactate as reactants.

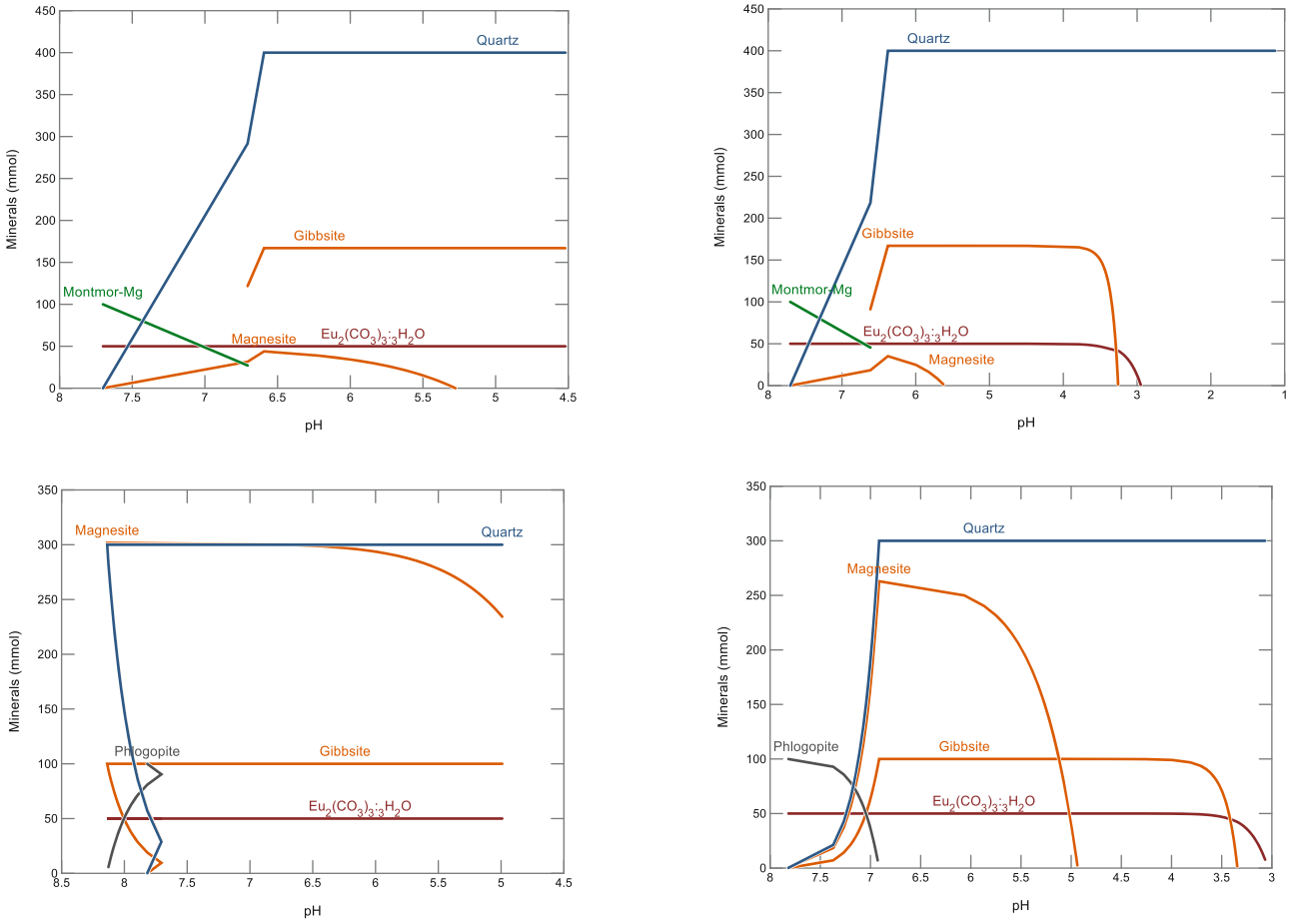

Figure 16: Modeling of (top) montmorillonite with Eu using (left) lactate (right) HCl + lactate as reactants; (bottom) phlogopite with Eu using (left) lactate (right) HCl + lactate as reactants.

4.2 Geochemical modeling of REE leaching from silicate minerals by organic acid

The first step of this modeling was, as with inorganic acid models, to equilibrate the silicate mineral and REE of interest with a dilute salt solution, prior to leaching commencing in the second step of modeling. The results of geochemical modeling (the trend of mineral dissolution) of leaching of chrysotile, forsterite, montmorillonite, and phlogopite with lactic acid and HCl are depicted in Figures 15–18. Looking at Figures 15–18, which present the pH-dependent data of the leaching step of the modeling, it is observed that the initial pH values of these systems were identical to those used for the inorganic acid systems. So again, only forsterite started at a higher pH close to 9, and the other silicates started at a pH close to 8.

Organic acids are characteristically weak acids, including lactic acid. Note that in these systems the reactant is named "lactate," which is the dissociated anion of lactic acid, but lactate was added alongside H^+ as a reactant, hence it behaves like lactic acid. Another way to prove that the lactate acted like lactic acid is to note that in these systems (without HCl), the final pH was limited since with reduced pH, lactic acid eventually reaches its dissociation equilibrium and stops dissociating. This limiting pH was between approximately 4.5 and 5.2, depending on the system. To enable the study of these systems under lower pH, simulations were done with the addition of HCl (a strong acid) as a co-lixiviant.

As with inorganic acids, the silicate minerals dissolved first in all cases as shown in Figures 15–18. The addition of the co-lixiviant did not significantly alter the pH-dependent dissolution. This is likely because the speciation of the dissolved species does not significantly involve chloride ions. In all cases, the REE carbonates did not dissolve in the systems using only lactic acid. For the forsterite and chrysotile systems, this is not an issue, since the REE solids are liberated, so they can be recovered in a single leaching step. In the montmorillonite and phlogopite systems, a second leaching step is

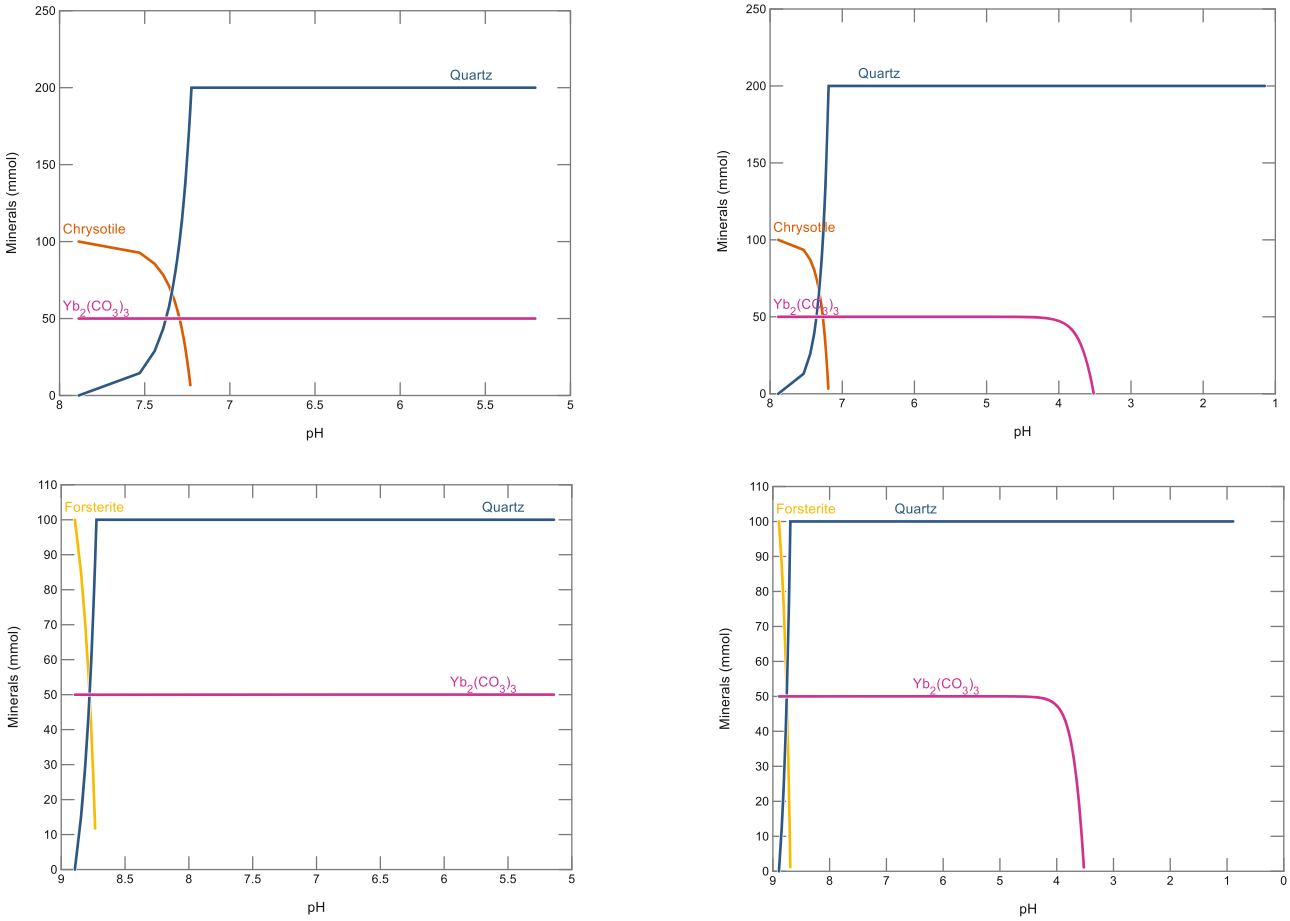

Figure 17: Modeling of (top) chrysotile with Yb using (left) lactate (right) HCl + lactate as reactants; (bottom) forsterite with Yb using (left) lactate (right) HCl + lactate as reactants.

needed to acidify the residual solids further. Figure 19 clarifies that the odd behavior of phlogopite in Figure 18, going forward and back, is due to the pH swinging down, then up, then down again, as lactate is added. When the mineral amounts are plotted versus lactate mass added (as in Figure 19), then the behavior is more as expected.

What is observed with the co-lixiviant HCl, which is different from the inorganic acid leaching models that used H_2SO_4, is that in a single leaching step, it is possible here to dissolve both the silicates and aluminum oxide before the Eu carbonates dissolve. In both cases, the Eu carbonate dissolved only when the pH reaches about 3.0, while the gibbsite dissolved at around 3.3–3.4. As before, the Eu carbonate proves to be more stable than the Yb carbonate, and this means that in a single leaching step with lactic acid and HCl, the Eu carbonate accumulates in the residual solid and can be recovered (together with quartz).

To investigate the validity of the modeling results, the stability diagrams of modeled minerals were plotted using the Act2 module of GWB (Figure 20). Accordingly, the REE carbonates dissolve in lower pHs ($Eu_2(CO_3)_3{:}3H_2O$ at pH ≤ 5.5 and $Yb_2(CO_3)_3$ at pH < 5). On the other hand, silicate minerals tend to dissolve at more neutral pH values (chrysotile at pH ≤ 7, forsterite at pH ≤ 8.5, Mg-montmorillonite at pH ≤ 6, and phlogopite at pH ≤ 6.5). These indications are not far from agreement with our results in terms of the pH range over which the REE carbonates (compared to silicate minerals) initiate to leach in the system.

Figure 21 summarizes the steps of recovery of REE carbonates using organic and inorganic acids investigated in this study. As discussed above, REEs can be recovered in all studied systems through 1-stage leachate using inorganic (sulfuric acid) and organic (lactic acid). The only exceptions are Mg-montmorillonite and phlogopite during bioleaching, requiring an additional step of adding HCl.

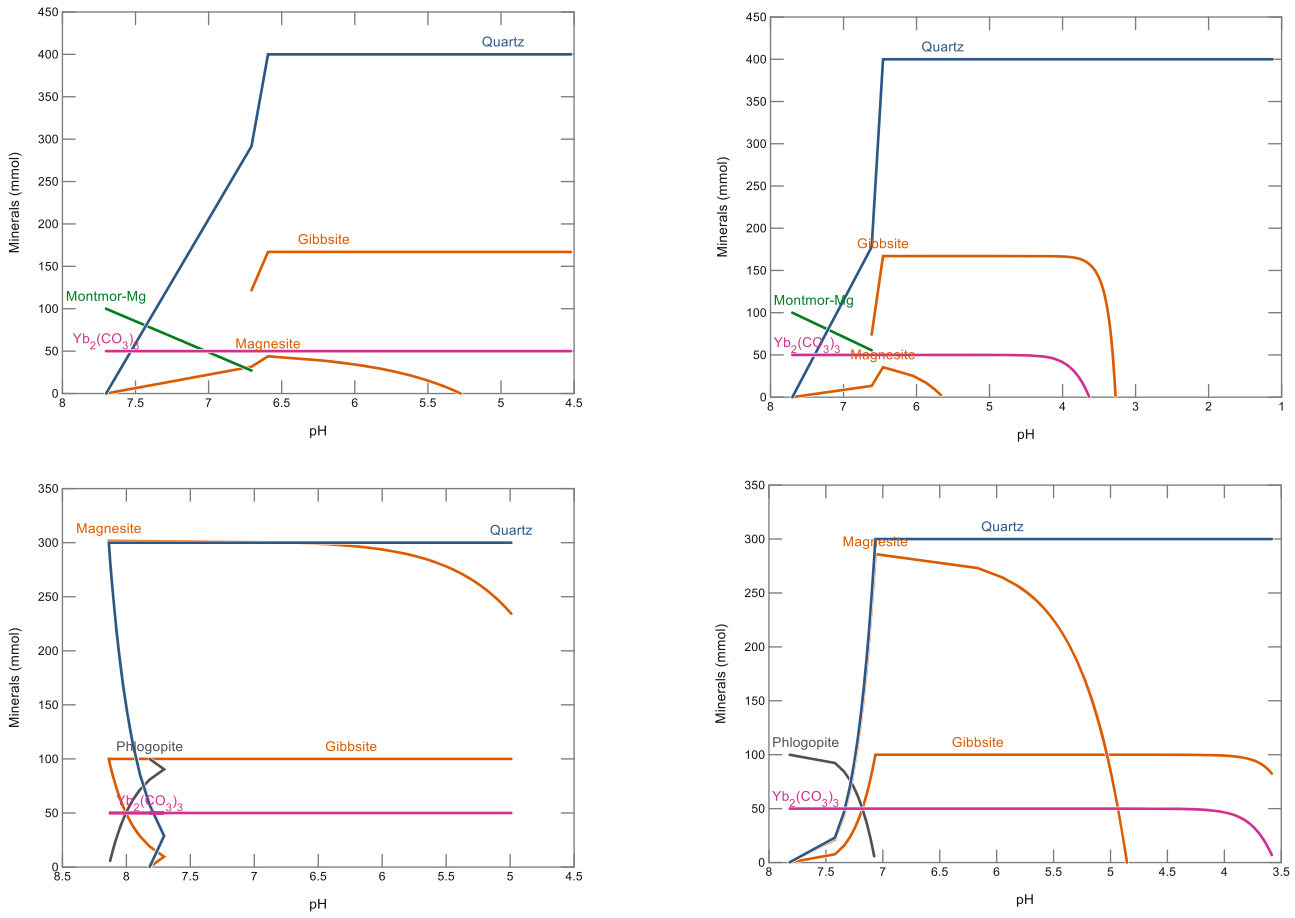

Figure 18: Modeling of (top) montmorillonite with Yb using (left) lactate (right) HCl + lactate as reactants; (bottom) phlogopite with Yb using (left) lactate (right) HCl + lactate as reactants.

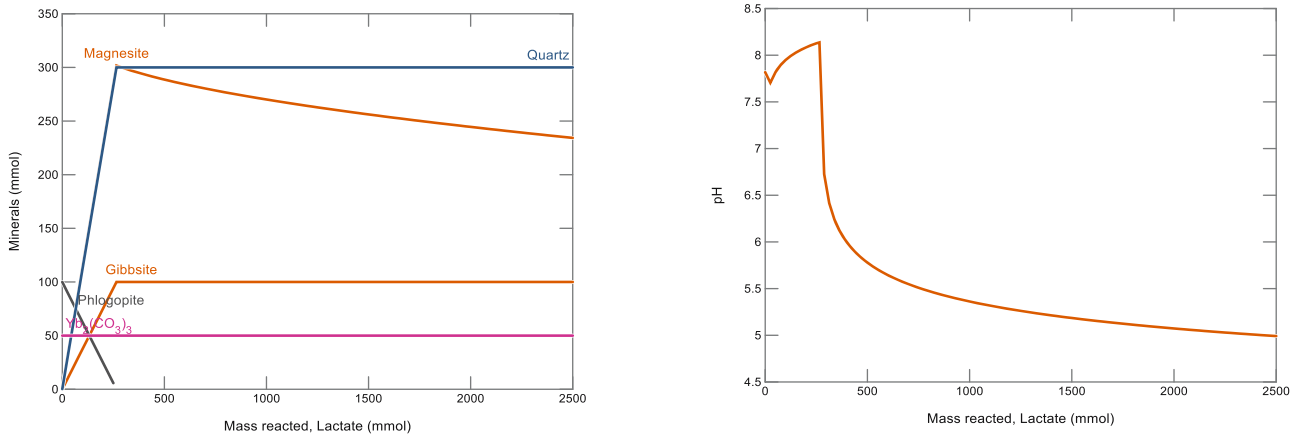

Figure 19: Modeling of phlogopite with Yb using lactate: mineral amounts versus lactate added (left), and pH versus lactate added (right).

5 Conclusions

REEs are typically found in low concentrations within natural rocks that make up mine tailings, such as carbonates in association with silicates within carbonatite igneous rocks, so it is of interest to develop (bio)hydrometallurgical ways to liberate them from the silicate matrix. The results of leachate with H_2SO_4 denote that this acid is sufficient to

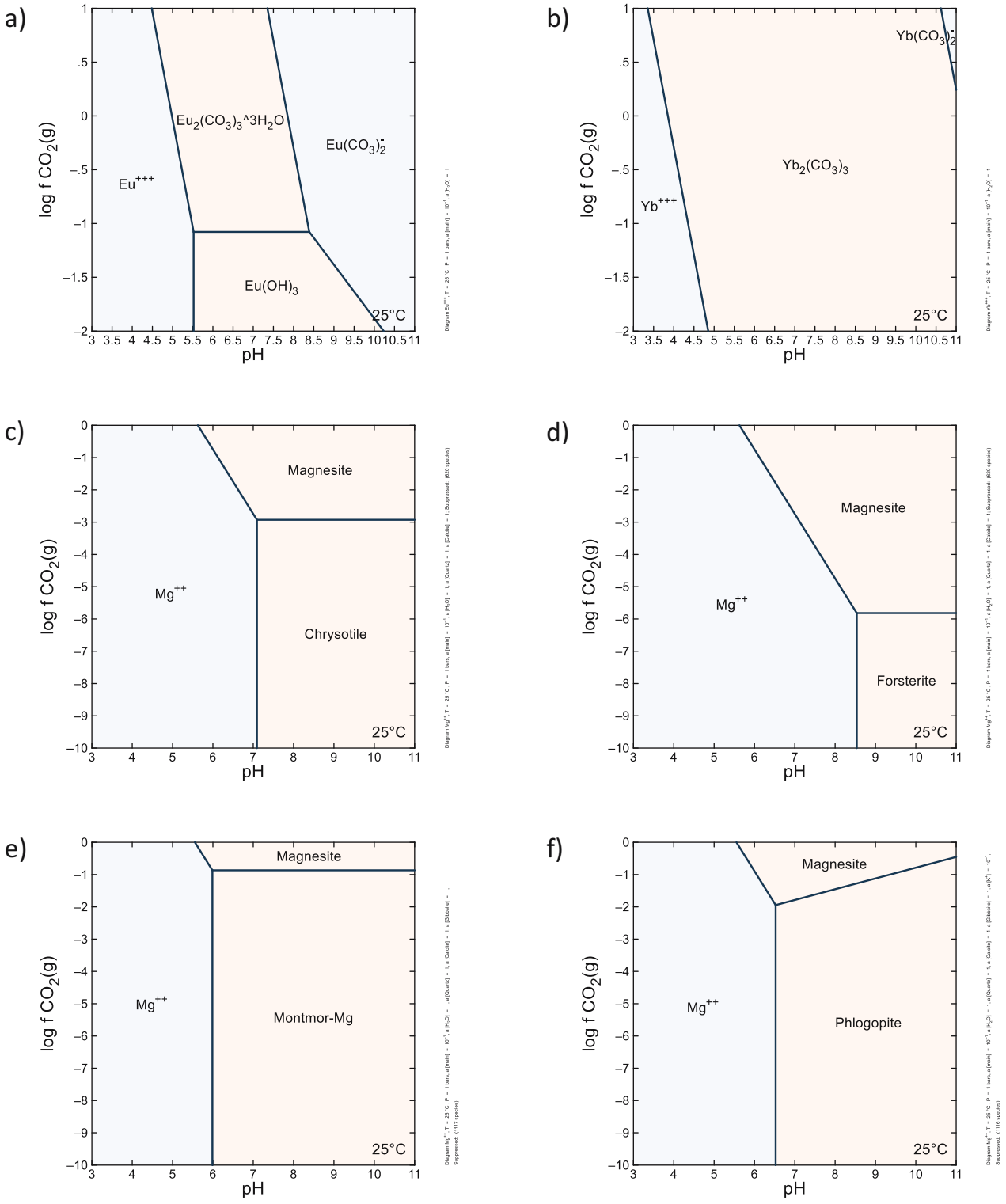

Figure 20: Stability diagram of modeled minerals (plotted in Act2 module of GWB): (a) $Eu_2(CO_3)_3{:}3H_2O$, (b) $Yb_2(CO_3)_3$, (c) chrysotile, (d) forsterite, (e) Mg-montmorillonite, and (f) phlogopite.

dissolve silicate mineral (forsterite at pH = 9 and other silicate minerals at pH 6–8) and REE carbonates (at pH 3–4) in different pH ranges. Focusing on organic acid (lactic acid), although this acid is capable of dissolving all silicate, there are two different behaviors for these minerals. The organic acid suffices to recover carbonates

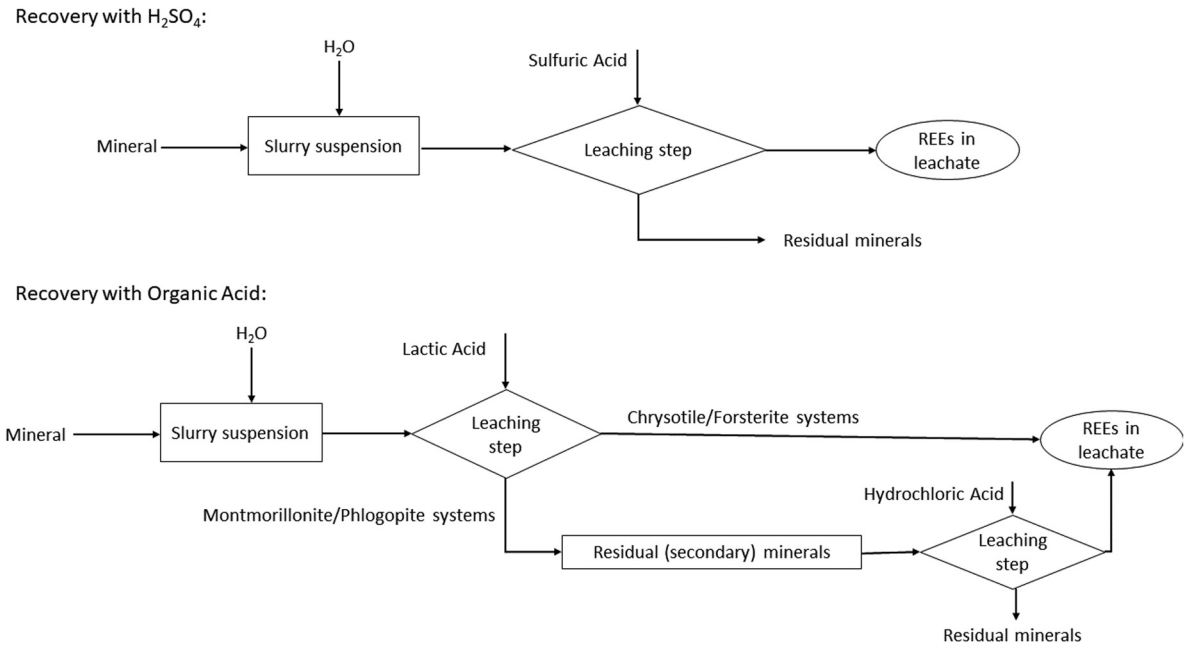

Figure 21: Summary of the leaching process of minerals investigated in this study using inorganic (sulfuric acid and hydrochloric acid) and organic (lactic acid) acids.

as REE solids are liberated during the dissolution of chrysotile and forsterite. However, an additional step of adding hydrochloric acid is required to recover REE carbonates in montmorillonite and phlogopite systems as residual solids of these minerals include secondary minerals that make the recovery of REE carbonates unattainable. In conclusion from the inorganic acid leaching models, REE carbonates are recoverable as solid particles that are liberated from the silicate matrix in rocks that contain forsterite and chrysotile, while REEs are recoverable in a secondary leaching step when they are initially contained in rocks made up of montmorillonite and phlogopite. In most cases, there is a sufficient pH difference between the initiation point of leaching of all minerals in these systems, so from a practical point of view, and to improve kinetics, it is possible to add extra acidity to accelerate leaching while still having some margin before the next mineral in the system starts to leach. The exception to this is the secondary leaching of Eu and Yb from gibbsite, where the pH difference between the conclusion of leaching of the former and the initiation of leaching of the latter is in the order of approximately 0.1–0.2 pH units. Reactive extraction of REEs during this secondary leaching (i.e., removing REEs from the solution while leaching is taking place) could be one way to avoid having to decrease the acidity too much.

In conclusion from the organic acid leaching models, REEs have the potential to be recovered from silicate rocks via bioleaching (microbial processes that produce organic acids), but the process configuration would differ depending on the predominant minerals that make up the rock, and the type of REE present in it. In some cases, bioleaching in a single step is sufficient, in other cases, two-step leaching, with bioleaching followed by chemical leaching, is required, and in other cases, bioleaching can be combined with chemical leaching in a single step. The variety of scenarios points to the need for substantial experimental work on the use of bioleaching to extract REEs from natural ores and industrial and urban wastes. Each solid and each REE will behave differently, and only experimentation can account for kinetic limitations, such as the rates of dissolution and precipitation of solid phases and the rate of diffusion of ionic species through solids. One limiting factor found during building up the modeling framework was that thermodynamic databases lack information for many REE carbonates. This could call for encouraging the researchers to develop a more comprehensive database for studying more REEs carbonate through geochemical modeling.

With growing worldwide interest in finding new sources of REEs and other CMs, there is a need to develop both new processes to extract REEs and CMs from natural minerals and waters, and also to recover REEs and CMs from industrial and urban wastes. In this thesis, these three topics were addressed. The approach taken involved reviewing scientific and industrial literature to survey the approaches already

attempted, and to identify the minerals and types of REEs and CMs that are relevant and important. In this way, it was identified that more work is needed on biological processes for the extraction of REEs from silicate minerals, and recovery of CMs from contaminated natural waters. Furthermore, it was identified that geochemical modeling is an attractive technique to be used as a proof-of-concept, as it relies on thermodynamic analysis of geochemical systems. Thermodynamically favorable processes are processes that deserve more attention in an experimental study, and thus geochemical modeling helps to identify the most promising processing routes of (bio)hydrometallurgy and bio-precipitation.

Funding information: The research leading to these results received funding from the Natural Sciences and Engineering Research Council of Canada (NSERC) under Grant Agreement No. 401497.

Author contributions: Nneka Joyce Odimba: writing – original draft, formal analysis; Reza Khalidy: writing – review and editing, formal analysis; Reza Bakhshoodeh: writing – original draft, writing – review and editing; Rafael M. Santos: methodology, writing – review and editing, project administration, resources.

Conflict of interest: The authors state no conflict of interest.

Other details: This article is based on a Master's thesis of Nneka Joyce Odimba entitled "Recovery of critical metals from urban and industrial wastes: a geochemical modeling investigation of (bio)hydrometallurgical leaching and bio-precipitation", published in January 2022 by the University of Guelph.

Data availability statement: All data generated or analyzed during this study are included in this published article and its supplementary information files.

References

[1] Majlessi M, Zamanzadeh M, Alavi N, Amanidaz N, Bakhshoodeh R. Generation rates and current management of municipal, construction and demolition wastes in Tehran. J Mater Cycles Waste Manag. 2019;21:191–200. doi: 10.1007/s10163-018-0772-z.

[2] Favot M, Massarutto A. Rare-earth elements in the circular economy: the case of yttrium. J Environ Manage. 2019;240:504–10. doi: 10.1016/j.jenvman.2019.04.002.

[3] Lieder M, Rashid A. Towards circular economy implementation: a comprehensive review in context of manufacturing industry. J Clean Prod. 2016;115:36–51. doi: 10.1016/j.jclepro.2015.12.042.

[4] Sabbas T, Polettini A, Pomi R, Astrup T, Hjelmar O, Mostbauer P, et al. Management of municipal solid waste incineration residues. Waste Manage. 2003;23(1):61–88. doi: 10.1016/S0956-053X(02)00161-7.

[5] Joseph AM, Snellings R, Van den Heede P, Matthys S, De, Belie N. The use of municipal solid waste incineration ash in various building materials: a Belgian point of view. Materials. 2018;11(1):141. doi: 10.3390/ma11010141.

[6] Wünsch C, Simon FG. The reduction of greenhouse gas emissions through the source-separated collection of household waste in Germany. In: Maletz R, Dornack C, Ziyang L, editors. Source separation and recycling. the handbook of environmental chemistry. Vol. 63. Cham: Springer; 2017. p. 19. doi: 10.1007/698_2017_35.

[7] Krook J, Svensson N, Eklund M. Landfill mining: a critical review of two decades of research. Waste Manage. 2012;32(3):513–20. doi: 10.1016/j.wasman.2011.10.015.

[8] Cossu R. Editorial: the urban mining concept. Waste Manage. 2013;33(3):497–8. doi: 10.1016/j.wasman.2013.01.010.

[9] Lu S, Sun S, Huang X, Tu G, Zhu X, Kong X. Optimization of recovering cerium from the waste polishing powder using response surface methodology. Green Process Synth. 2017;6(2):217–24. doi: 10.1515/gps-2016-0030.

[10] Das S, Natarajan G, Ting YP. Bio-extraction of precious metals from urban solid waste. AIP Conference Proceedings. 2017;1805:020004. doi: 10.1063/1.4974410.

[11] Habibi A, Kourdestani SS, Hadadi M. Biohydrometallurgy as an environmentally friendly approach in metals recovery from electrical waste: a review. Waste Manage Res. 2020;38(3):232–44. doi: 10.1177/0734242X19895321.

[12] Weng Z, Jowitt SM, Mudd GM, Haque N. A detailed assessment of global rare earth element resources: opportunities and challenges. Econ Geol. 2015;110(8):1925–52. doi: 10.2113/econgeo.110.8.1925.

[13] Xie Y, Hou Z, Goldfarb RJ, Guo X, Wang L. Rare earth element deposits in China. In: Verplanck PL, Hitzman MW, editors. Rare earth and critical elements in ore deposits. McLean, VA, USA: Society of Economic Geologists; 2016. doi: 10.5382/Rev.18.06.

[14] Xu C, Kynický J, Smith M, Kopriva A, Brtnický M, Urubek T, et al. Origin of heavy rare earth mineralization in South China. Nat Commun. 2017;8:14598. doi: 10.1038/ncomms14598.

[15] Edahbi M, Plante B, Benzaazoua M, Pelletier M. Geochemistry of rare earth elements within waste rocks from the Montviel carbonatite deposit, Québec, Canada. Environ Sci Pollut Res. 2018;25:10997–1010. doi: 10.1007/s11356-018-1309-7.

[16] Gómez-Arias A, Yesares L, Díaz J, Caraballo MA, Maleke M, Sáez R, et al. Mine waste from carbonatite deposits as potential rare earth resource: insight into the Phalaborwa (Palabora) Complex. J Geochem Explor. 2022;232:106884. doi: 10.1016/j.gexplo.2021.106884.

[17] Yun Y, Stopic S, Friedrich B. Valorization of rare earth elements from a steenstrupine concentrate via a combined hydrometallurgical and pyrometallurgical method. Minerals. 2020;10:248. doi: 10.3390/min10030248.

[18] Fathollahzadeh H, Eksteen JJ, Kaksonen AH, Watkin EL. Role of microorganisms in bioleaching of rare earth elements from

primary and secondary resources. Appl Microb Biotechnol. 2019;103(3):1043–57. doi: 10.1007/s00253-018-9526-z.
[19] Khalidy R, Santos RM. Assessment of geochemical modeling applications and research hot spots – a year in review. Environ Geochem Health. 2021;43(9):3351–74. doi: 10.1007/s10653-021-00862-w.
[20] Araujo F, Fantucci H, Nunes E, Santos RM. Geochemical modeling applied in waste disposal, and its relevance for municipal solid waste management. Minerals. 2020;10(10):846. doi: 10.3390/min10100846.
[21] Das N, Das D. Recovery of rare earth metals through biosorption: an overview. J Rare Earths. 2013;31:933–43. doi: 10.1016/S1002-0721(12)60382-2.
[22] Xie F, Zhang TA, Dreisinger D, Doyle F. A critical review on solvent extraction of rare earths from aqueous solutions. Min Eng. 2014;56:10–28. doi: 10.1016/j.mineng.2013.10.021.
[23] Zhuang WQ, Fitts JP, Ajo-Franklin CM, Maes S, Alvarez-Cohen L, Hennebel T. Recovery of critical metals using biometallurgy. Curr Opin Biotechnol. 2015;33:327–35. doi: 10.1016/j.copbio.2015.03.019.
[24] Cheremisina OV, Volkova O, Litvinova TE. Influence of anion nature on acid leaching of silicate minerals and solvent extraction of rare and rare-earth elements. Geochemistry. 2020;80:125507. doi: 10.1016/j.chemer.2019.04.003.
[25] Dodson JR, Hunt AJ, Parker HL, Yang Y, Clark JH. Elemental sustainability: towards the total recovery of scarce metals. Chem Eng Process. 2012;51:69. doi: 10.1016/j.cep.2011.09.008.
[26] Du X, Graedel TE. Global in-use stocks of the rare earth elements: a first estimate. Environ Sci Technol. 2011;45:4096. doi: 10.1021/es102836s.
[27] Yano J, Muroi T, Sakai SI. Rare earth element recovery potentials from end-of-life hybrid electric vehicle components in 2010–2030. J Mat Cycl Waste Manag. 2016;18(4):655–64. doi: 10.1007/s10163-015-0360-4.
[28] Li Y, Fujikawa K, Wang J, Li X, Ju Y, Chen C. The potential and trend of end-of-life passenger vehicles recycling in China. Sustainability. 2020;12(4):1455. doi: 10.3390/su12041455.
[29] Hoenderdaal S, Espinoza LT, Marscheider-Weidemann F, Graus W. Can a dysprosium shortage threaten green energy technologies? Energy. 2013;49:344–55. doi: 10.1016/j.energy.2012.10.043.
[30] Alonso E, Sherman AM, Wallington TJ, Everson MP, Field FR, Roth R, et al. Evaluating rare earth element availability: a case with revolutionary demand from clean technologies. Environ Sci Technol. 2012;46(6):3406–14. doi: 10.1021/es203518d.
[31] Wen ZP, Zhou CC, Pan JH, Cao S, Hu T, Ji W, et al. Recovery of rare-earth elements from coal fly ash via enhanced leaching. Int J Coal Prep Util. 2022;42(7):2041–55. doi: 10.1080/19392699.2020.1790537.
[32] Middleton A, Park DM, Jiao Y, Hsu-Kim H. Major element composition controls rare earth element solubility during leaching of coal fly ash and coal by-products. Int J Coal Geol. 2020;227:103532. doi: 10.1016/j.coal.2020.103532.
[33] Odimba N, Santos RM. Application of geochemical modeling in rare earth elements leaching of coal combustion and secondary residues. In: Jyothi RK, Parhi PK, editors. Clean coal technologies. Springer Nature; 2021. p. 605–16. doi: 10.1007/978-3-030-68502-7_24.
[34] Wang Z, Dai SF, Zou JH, French D, Graham IT. Rare earth elements and yttrium in coal ash from the Luzhou power plant in Sichuan, Southwest China: concentration, characterization and optimized extraction. Int J Coal Geol. 2019;203:1–14. doi: 10.1016/j.coal.2019.01.001.
[35] Vass CR, Noble A, Ziemkiewicz PF. The occurrence and concentration of rare earth elements in acid mine drainage and treatment by-products: Part 1 – initial survey of the northern appalachian coal basin. Min Metall Explor. 2019;36:903–16. doi: 10.1007/s42461-019-0097-z.
[36] Honaker RQ, Groppo J, Yoon R-H, Luttrell GH, Noble A, Herbst J. Process evaluation and flowsheet development for the recovery of rare earth elements from coal and associated byproducts. Min Metall Process. 2017;34(3):107–15. doi: 10.19150/mmp.7610.
[37] Zhang W, Honaker RQ. Rare earth elements recovery using staged precipitation from leachate generated from coarse coal refuse. Int J Coal Geol. 2018;195:189–99. doi: 10.1016/j.coal.2018.06.008.
[38] Sarswat PK, Leake M, Allen L, Free ML, Hu X, Kim D, et al. Efficient recovery of rare earth elements from coal based resources: a bioleaching approach. Mater Today Chem. 2020;16:100246. doi: 10.1016/j.mtchem.2020.100246.
[39] Alkan G, Schier C, Gronen L, Stopic S, Friedrich B. A mineralogical assessment on residues after acidic leaching of bauxite residue (Red Mud) for titanium recovery. Metals. 2017;7:458. doi: 10.3390/met7110458.
[40] Qu Y, Li H, Wang X, Tian W, Shi B, Yao M, et al. Bioleaching of major, rare earth, and radioactive elements from red mud by using indigenous chemoheterotrophic bacterium *Acetobacter* sp. Minerals. 2019;9:67. doi: 10.3390/min9020067.
[41] Zhang R, Zheng S, Ma S, Zhang Y. Recovery of alumina and alkali in Bayer red mud by the formation of andradite-grossular hydrogarnet in hydrothermal process. J Hazard Mater. 2011;189:827–35. doi: 10.1016/j.jhazmat.2011.03.004.
[42] Bonomi C, Alexandri A, Vind J, Panagiotopoulou A, Tsakiridis P, Panias D. Scandium and titanium recovery from bauxite residue by direct leaching with a bronsted acidic ionic liquid. Metals. 2018;8:834. doi: 10.3390/met8100834.
[43] Cao S, Zhou C, Pan J, Liu C, Tang M, Ji W, et al. Study on influence factors of leaching of rare earth elements from coal fly ash. Energy Fuels. 2018;32(7):8000–5. doi: 10.1021/acs.energyfuels.8b01316.
[44] Franus W, Wiatros-Motyka MM, Wdowin M. Coal fly ash as a resource for rare earth elements. Environ Sci Pollut Res. 2015;22(12):9464–74. doi: 10.1007/s11356-015-4111-9.
[45] Taggart RK, Hower JC, Dwyer GS, Hsu-Kim H. Trends in the rare earth element content of U.S.-based coal combustion fly ashes. Environ Sci Technol. 2016;50(11):5919–26. doi: 10.1021/acs.est.6b00085.
[46] Yang X, Honaker RQ. Leaching kinetics of rare earth elements from fire clay seam coal. Minerals. 2020;10:491. doi: 10.3390/min10060491.
[47] Li Z, Xie Z, He D, Deng J, Zhao H, Li H. Simultaneous leaching of rare earth elements and phosphorus from a Chinese phosphate ore using H_3PO_4. Green Process Synth. 2021;10(1):258–67. doi: 10.1515/gps-2021-0023.
[48] Cen P, Wu W, Bian X. A novel process for recovery of rare earth and fluorine from bastnaesite concentrates. Part I:

calcification roasting decomposition. Green Process Synth. 2016;5(4):427–34. doi: 10.1515/gps-2016-0031.
[49] Kashiwakura S, Kumagai Y, Kubo H, Wagatsuma K. Dissolution of rare earth elements from coal fly ash particles in a dilute H_2SO_4 solvent. Open J Phys Chem. 2013;3(2):69–75. doi: 10.4236/ojpc.2013.32009.
[50] Kolker A, Scott C, Hower JC, Vazquez JA, Lopano CL, Dai S. Distribution of rare earth elements in coal combustion fly ash, determined by SHRIMP-RG ion microprobe. Int J Coal Geol. 2017;184:1–10. doi: 10.1016/j.coal.2017.10.002.
[51] Lin R, Bank TL, Roth EA, Granite EJ, Soong Y. Organic and inorganic associations of rare earth elements in central Appalachian coal. Int J Coal Geol. 2017;179:295–301. doi: 10.1016/j.coal.2017.07.002.
[52] Dai S, Zhao L, Hower JC, Johnston MN, Song W, Wang P, et al. Petrology, mineralogy, and chemistry of size-fractioned fly ash from the Jungar power plant, Inner Mongolia, China, with emphasis on the distribution of rare earth elements. Energy Fuels. 2014;28(2):1502–14. doi: 10.1021/ef402184t.
[53] Dai S, Zhou Y, Zhang M, Wang X, Wang J, Song X, et al. A new type of Nb (Ta)–Zr(Hf)–REE–Ga polymetallic deposit in the late Permian coal-bearing strata, eastern Yunnan, southwestern China: possible economic significance and genetic implications. Int J Coal Geol. 2010;83(1):55–63. doi: 10.1016/j.coal.2010.04.002.
[54] Blissett RS, Smalley N, Rowson NA. An investigation into six coal fly ashes from the United Kingdom and Poland to evaluate rare earth element content. Fuel. 2014;119:236–9. doi: 10.1016/j.fuel.2013.11.053.
[55] Yakaboylu GA, Baker D, Wayda B, Sabolsky K, Zondlo JW, Shekhawat D, et al. Microwave-assisted pretreatment of coal fly ash for enrichment and enhanced extraction of rare-earth elements. Energy Fuels. 2019;33(11):12083–95. doi: 10.1021/acs.energyfuels.9b02846.
[56] Lin G, Zhang L, Yin S, Peng J, Li S, Xie F. Study on the calcination experiments of rare earth carbonates using microwave heating. Green Process Synth. 2015;4(4):329–36. doi: 10.1515/gps-2015-0040.
[57] Ghorbani Y, Oliazadeh M, Shahverdi AR. Microbiological leaching of al from the waste of Bayer process by some selective fungi. Iran J Chem Chem Eng. 2009;28(1):109–15. doi: 10.30492/IJCCE.2009.6922.
[58] Chiang YW, Santos RM, Van Audenaerde A, Monballiu A, Van Gerven T, Meesschaert B. Chemoorganotrophic bioleaching of olivine for nickel recovery. Minerals. 2014;4:553–64. doi: 10.3390/min4020553.
[59] Guezennec AG, Joulian C, Jacob J, Archane A, Ibarra D, Gregory R, et al. Influence of dissolved oxygen on the bioleaching efficiency under oxygen enriched atmosphere. Min Eng. 2017;106:64–70. doi: 10.1016/j.mineng.2016.10.016.
[60] Zhu W, Xia J-I, Yang Y, Nie Z-Y, Peng A-A, Liu H-C, et al. Thermophilic archaeal community succession and function change associated with the leaching rate in bioleaching of chalcopyrite. Bioresour Technol. 2013;133:405–13. doi: 10.1016/j.biortech.2013.01.135.
[61] Bosecker K. Bioleaching: metal solubilization by microorganisms. FEMS Microbiol Rev. 1997;20:591–604. doi: 10.1111/j.1574-6976.1997.tb00340.
[62] Tuovinen OH, Kelly DP. Studies on the growth of *Thiobacillus ferrooxidans* I. Use of membrane filters and ferrous iron agar to determine viable numbers, and comparison with $^{14}CO_2$-fixation and iron oxidation as measures of growth. Arch Microbiol. 1973;88:285–98.
[63] Maluckov BS. The catalytic role of *Acidithiobacillus ferrooxidans* for metals extraction from mining – metallurgical resource. Biodivers Int J. 2017;1(3):109–19. doi: 10.15406/bij.2017.01.00017.
[64] Torma AE, Walden CC, Branion RMR. Microbiological leaching of a zinc concentrate. Biotechnol Bioeng. 1970;12:501–17.
[65] Bosecker K. Studies on the bacterial leaching of nickel ores. In: Schwartz W, editor. Conference Bacterial Leaching. Weinheim: Verlag Chemie; 1977. p. 139–44.
[66] Torma AE. The role of *Thiobacillus ferrooxidans* in hydrometallurgical processes. Adv Biochem Eng. 1977;6:1–37.
[67] Pradhan N, Nathsarma KC, Srinivasa R, Sukla LB, Mishra BK. Heap bioleaching of chalcopyrite: a review. Min Eng. 2008;21:355–65. doi: 10.1016/j.mineng.2007.10.018.
[68] Leahy MJ, Davidson MR, Schwarz MP. A model for heap bioleaching of chalcocite with heat balance: bacterial temperature dependence. Min Eng. 2005;18:1239–52. doi: 10.1016/j.mineng.2005.07.003.
[69] Jafari M, Shafaei SZ, Abdollahi H, Gharabaghi M, Chehreh Chelgani S. Effect of flotation reagents on the activity of *L. ferrooxidans*. Min Process Extr Metall Rev. 2018;39(1):34–43. doi: 10.1080/08827508.2017.1323748.
[70] Zhao H, Zhang Y, Zhang X, Qian L, Sun M, Yang Y, et al. The dissolution and passivation mechanism of chalcopyrite in bioleaching: an overview. Miner Eng. 2019 Jun;136:140–54. doi: 10.1016/j.mineng.2019.03.014.
[71] Chiang YW, Santos RM, Monballiu A, Ghyselbrecht K, Martens JA, Mattos ML, et al. Effects of bioleaching on the chemical, mineralogical and morphological properties of natural and waste-derived alkaline materials. Miner Eng. 2013 Jul;48:116–25. doi: 10.1016/j.mineng.2012.09.004.